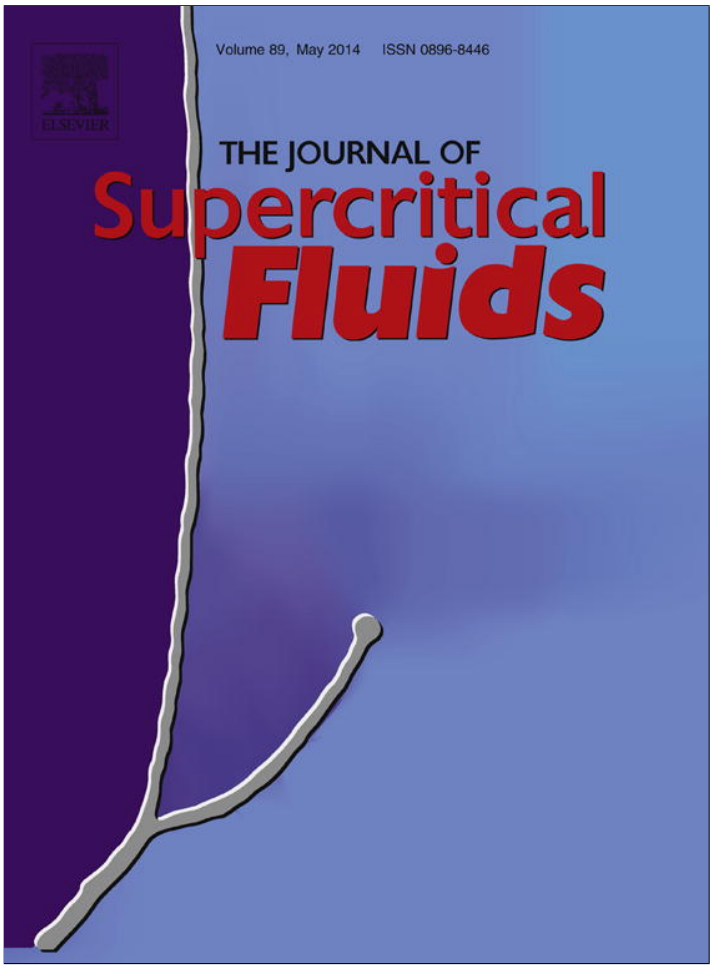

J. of Supercritical Fluids 89 (2014) 33–47

Contents lists available at ScienceDirect

The Journal of Supercritical Fluids

journal homepage: www.elsevier.com/locate/supflu

Critical end line topologies for ternary systems

G. Pisoni[a,b,c], M. Cismondi[b,c], L. Cardozo-Filho[d], M.S. Zabaloy[a,*]

[a] Planta Piloto de Ingeniería Química - Universidad Nacional del Sur – CONICET CC 717 - 8000 Bahía Blanca, Prov. Buenos Aires, Argentina
[b] IDTQ-Grupo Vinculado PLAPIQUI – CONICET, Argentina
[c] Facultad de Ciencias Exactas Físicas y Naturales, Universidad Nacional de Córdoba – Av. Vélez Sarsfield 1611, Ciudad Universitaria, X5016GCA Córdoba, Argentina
[d] Departmento de Engenharia Quimica, Universidad Estadual de Maringá, 87020-900 Maringá, PR, Brazil

ARTICLE INFO

Article history:
Received 21 May 2013
Received in revised form 22 January 2014
Accepted 22 January 2014
Available online 14 February 2014

Keywords:
Critical end lines
Ternary systems
Equation of state

ABSTRACT

A ternary critical end line (T-CEL) is a line of Ternary critical end points (T-CEPs). T-CELs provide key information on the phase behavior of ternary systems, i.e., they are boundaries for the ternary three-phase equilibrium. A ternary system may have several T-CELs. It is desirable to have available a robust algorithm for computing complete ternary CELs, thus minimizing the need for user intervention. It is also important to reliably detect the key points where T-CELs originate or terminate. In this work, we propose to apply a numerical continuation method (NCM) for the fast and robust computation of T-CELs. We present calculated T-CELs for highly asymmetric systems showing the topologies that these lines define. We consider a model of the equation of state (EOS) type and use it over wide ranges of conditions. Such ranges are much wider than those previously considered in the literature. Our main conclusion is that models for the fluid phase equilibria of ternary systems may predict, for a given system, several T-CELs of varying types and topologies. Some of such topologies have been observed for the first time in this work.

1. Introduction

The computation of the fluid phase equilibrium behavior of binary and ternary systems is of great importance to characterize the behavior of models and their specified parameter values, as a necessary step to intend the reproduction of experimental information by the chosen model. Such characterization is best carried out when focusing on key equilibrium lines and points.

The key lines and points for the fluid phase equilibria of binary systems are those identified by Scott and Van Konynenburg in 1970 [1], i.e., critical, azeotropic and liquid–liquid–vapor lines, critical end points and a variety of end points for azeotropic lines. The mentioned lines are actually non-linear and would therefore be named "curves" by a mathematician (ref [2], p. 114). In other words, critical, azeotropic and liquid–liquid–vapor lines are understood to be curves [2]. "Only tie lines are straight lines" [2].

In ternary systems, an important type of, in a way, key point, is the (ternary) critical end point (T-CEP). At a T-CEP a critical fluid phase is at equilibrium with a non-critical fluid phase, being the system made of three components. A T-CEP is the termination of a ternary three-phase equilibrium line. This line may be, e.g., isothermal or isobaric.

Appendix C presents a significant part of the phenomenology relevant to this work for the fluid phase behavior of ternary mixtures. Three and four-phase equilibria, critical lines and T-CEPs are represented together with other phase equilibrium objects in the familiar Gibbs triangles. Appendix C is mostly based on the comprehensive review by Adrian et al. [3]. Notice that after section 6, both, a list of acronyms and a list of symbols are provided.

For computing a T-CEP it is necessary to add, to the critical conditions, the isofugacity conditions between the critical and non-critical phases (Appendix A). The resulting system of equations (SE) has only one degree of freedom. Therefore, the T-CEP conditions define one or more continuous lines (or hyper-lines) of T-CEPs for a given ternary system, model, and parameter values. A proper name for a line of T-CEPs is "ternary critical end line" (T-CEL). Notice that a T-CEL is a T-CEP locus. A T-CEL (actually a hyper-line) is a characteristic univariant line of a ternary system. At a T-CEL, a three-phase hyper-surface and a critical hyper-surface meet. A T-CEL is indeed a key line whose computation makes possible to facilitate the systematic evaluation of a combination of a chosen model and a set of specified values for its parameters. A ternary system may have from none to several T-CELs. As it is the case for binary univariant lines, a ternary critical end line (or hyper-line) is understood to be a curve (or hyper-curve) despite the use of the word "line".

* Corresponding author.
E-mail addresses: mzabaloy@plapiqui.edu.ar, marcelo.zabaloy@yahoo.com.ar (M.S. Zabaloy).

0896-8446/$ – see front matter © 2014 Elsevier B.V. All rights reserved.
http://dx.doi.org/10.1016/j.supflu.2014.01.014

List of symbols

$\hat{f}_i$	fugacity of component i in the mixture
I	identity matrix
$J_{F^{(15)}}$	Jacobian matrix of vector function $F^{(15)}$
M^*_{ij}	element of matrix $\mathbf{M}^*$
n_i	number of moles of component i (ith element of vector $\mathbf{n}$)
$\mathbf{n}$	number of moles vector
P	absolute pressure
P^*	logarithmically scaled P
R	universal gas constant
s	distance parameter
S_{spec}	value assigned to the specified variable
T	absolute temperature
T^*	logarithmically scaled T
tpd	tangent plane distance function
u_i	ith element of eigenvector $\mathbf{u}$
$\mathbf{u}$	eigenvector of matrix $\mathbf{M}^*$
v^0	molar volume of the critical phase
v^{0^*}	logarithmically scaled v^0
V^*	logarithmically scaled V
V_x	molar volume of the non-critical phase
V_x^*	logarithmically scaled V_x
x_i	mole fraction of component i in the non-critical phase
x_i^*	logarithmically scaled x_i
$\mathbf{x}$	mole fraction vector, with elements x_i.
z_i	mole fraction of component i in the critical phase
z_i^*	logarithmically scaled z_i
$\mathbf{z}$	mole fraction vector, with elements z_i.
ΔS_{spec}	change in parameter S_{spec}
λ	eigenvalue associated to the eigenvector $\mathbf{u}$
Λ_s	specified variable
$\Lambda^0_{next\ point}$	initial estimate for the vector Λ of the next point of the T-CEL
$\Lambda_{conv.point}$	vector Λ of a converged point of a T-CEL

List of Acronyms

15D	having fifteen dimensions
2D	having two dimensions
3D	having three dimensions
4PE	four phase equilibrium
B-CEP	binary critical end point
EOS	equation of state
inf-T-CEP	T-CEP where one of the components is at infinite dilution
NCM	numerical continuation method
P-CP	pure (compound) critical point
PR-EOS	Peng-Robinson equation of state
SRK-EOS	Sove-Redlich-Kwong equation of state
T-4PL	ternary four phase (equilibrium) line
T-CEL	ternary critical end line
T-CEP	ternary critical end point
T-CEP-4PL	ternary critical end point of a four phase line
T-TCEP	ternary tricritical end point

It is worth noting that we use the word "hyper-line" to identify a continuous set of points, each characterized by several coordinates, being defined, each point, by a single degree of freedom. A hyper-line has several projections, i.e., a hyper-line has an associated set of elementary curves that can be represented in a corresponding set of 2D diagrams. Besides, in this work we use the word "hyper-surface" to identify a continuous set of points, each characterized by several coordinates, being defined, each point, by two degrees of freedom. A hyper-surface has an associated set of elementary surfaces: they are the projections of the hyper-surface and can be represented in a corresponding set of 3D diagrams. Notice that the prefix "hyper" means in this work "several (more than three) coordinates". Levelt-Sengers ([2], p. 46) has referred to ternary "critical surfaces", while Gauter et al. [4] have considered both, critical and three-phase ternary "surfaces". In spite of the glossary of refs [2] and [4], we often prefer to add the prefix "hyper" to the word "surface" (or "line") to bear in mind the multidimensionality of the thermodynamic objects of interest. For instance, on page 135 of ref [4], a ternary (CO_2 + 1-octanol + hexadecane) "critical surface" is represented in the 3D space of variables pressure, temperature and solvent-free mass fraction of a component (Fig. 7 of ref [4]). In such figure, the pressure is the dependent variable. However, an analogous plot would exist if the critical pressure were exchanged by, e.g., the density of the critical phase. Thus, several 3D ternary critical surfaces are all contained within a single critical hyper-surface. This justifies the use of the prefix "hyper". Actually, Fig. 7 of ref [4] shows only one of the several possible 3D projections of a critical hyper-surface of system CO_2 + 1-octanol + hexadecane.

Di Andreth [5] studied the ternary system *CO_2 + water + 2-propanol*, and developed a couple of algorithms: one for computing ternary three-phase equilibria, and another one for calculating ternary four-phase equilibria. Di Andreth [5] showed T-CELs, computed with the Peng-Robinson EOS [PR-EOS, [6]], but did not provide detailed information on the calculation procedure for T-CEPs. According to the phase rule, a ternary three-phase equilibrium has two degrees of freedom (ref [2], p. 46). When one of them is spent, e.g., by setting a constant temperature, a three-phase equilibrium hyper-line, i.e., a continuous set of three-phase equilibria, becomes defined, e.g., an isothermal three-phase hyper-line. It seems that, in ref [5], each T-CEP of a given T-CEL would be identified while calculating a three-phase equilibrium hyper-line when verifying the absence of convergence. In other words, and in contrast with this work, Di Andreth [5] did not compute T-CEPs in a direct way.

Gregorowicz and de Loos [7] have presented calculated T-CELs for *methane + propane + n-eicosane* and *ethane + propane + n-eicosane*. They have suggested to start off by computing the critical end points of the binary subsystems (B-CEPs), and next to use such information to initialize the computation of a number of T-CEPs equal to the number of B-CEPs. However, the authors have not provided details on how to initialize the T-CEP variables that do not exist in a B-CEP, which is located very close to the T-CEP to be computed. Such variables are the concentrations of the third component in the two equilibrium phases of the T-CEP. A T-CEP located very close to a B-CEP is an infinite dilution T-CEP, since the concentration of one of the three components, in either equilibrium phase, tends to zero. Besides, Gregorowicz and de Loos [7] have suggested to set the temperature as the independent variable in the computation of T-CEPs. Such choice might not be a convenient one if the T-CEL, to which the T-CEPs being computed belong, has a highly non-linear behavior. Specifying a value for temperature is not appropriate in parts of T-CELs where the temperature remains practically constant, or it changes slowly [e.g., T-CEL(d) in Fig. 5].

Adrian et al. [8] experimentally studied, at varying temperatures and pressures, three-phase and four-phase equilibria, and CEPs, for the ternary system *CO_2 + H_2O + 1-propanol*. They [8] presented several qualitative diagrams to explain the observed phase behavior. Besides, they [8] showed quantitative diagrams which present both, experimental data and modeling results. These phase diagrams include typical triangular diagrams at set temperature and pressure, and pressure versus mole fraction (or density) projections of three-phase equilibrium lines. Adrian et al. [8] did not describe the calculation algorithms that they used to generate their modeling results.

Later, Adrian et al. [3] studied a large number of *CO_2 + H_2O + polar solvent* systems. They modeled the phase behavior of the ternary systems using the PR-EOS [6] coupled to a number of mixing rules. The authors presented qualitative and quantitative diagrams. The later ones showed Pressure-Temperature projections of calculated T-CELs, together with lines of other natures. Adrian et al. [3] reported that they had calculated the T-CELs using a numerical continuation method, but did not describe in detail its implementation. They did not provide either information on how a first converged point of a given T-CEL would be obtained. Adrian et al. [8] and Adrian et al. [3] did not provide discussions on the possible behaviors that T-CELs may show, but they [8] emphasized the importance of T-CELs as boundaries of three-phase equilibrium hyper-surfaces.

Winkler and Stephan [9] reported experimental T-CEPs and four-phase equilibria for the system CO_2 + H_2O + 1-butanol. They modeled such system using the Soave-Redlich-Kwong equation of state (SRK-EOS) [10] coupled to a number of mixing rules, but did not provide details on calculation procedures for T-CEPs or T-CELs. Similarly, no discussion is available in ref [9] on the possible end points for T-CELs.

Chobanov et al. [11] reported experimental T-CEPs for systems of the type CO_2 + alkanol + hydrophobic ionic liquid. For the case of CO_2 + methanol + [bmim][PF6], the authors presented a qualitative pressure-temperature projection of T-CELs and of other binary and unary hyper-lines.

Ulanova et al. [12] reported experimental T-CEPs for the systems *ethane + water + acetone* and *ethene + water + acetone* and modeled their behavior coupling a cubic equation of state to a number of mixing rules. The authors did no provide calculation procedures. On the other hand, Ulanova et al. [13] had previously reported experimental T-CEPs for ethene + water + 2-propanol without attempting to model them.

Freitag et al. [14] studied the systems *ethene + water + 1-propanol* and *ethene + water + 2-propanol*, for which they reported experimental T-CEPs over wide ranges of pressure and temperature. The modeling was carried out in ref [15] using the PR-EOS [6].

In refs [12] and [15] the work of Adrian et al. [3] is quoted as the source of more details on the calculation algorithms used.

Bluma and Deiters [16] have proposed a classification for the fluid phase behavior of ternary systems, showing the connection between the behavior of ternary critical surfaces and the phase behavior of the binary sub-subsystems that constitute the ternary system. Bluma and Deiters [16] referred to T-CELs as boundaries for the critical surfaces. However, they covered cases where the topology of the T-CELs can be regarded, in relative terms, as simple. This simplicity is inherited by the critical surfaces associated to the simple T-CELs. No discussion is provided in ref [16] on the behavior of the critical surfaces for cases, as some of those that will be shown later in this work, where the T-CELs have a complex behavior. Finally, Bluma and Deiters [16] did not discuss how the T-CELs can be calculated.

From the previous paragraphs it is concluded that the computation of T-CELs has not been described with enough detail in the literature. Besides, it seems that not all possible types of T-CELs have been identified in previous works. In such works, the computations seem to have always been limited to ranges of conditions narrower than those that can be covered by the models chosen for describing the behavior of the fluid system.

In this work, we propose to apply a numerical continuation method (NCM) for the fast and robust computation of ternary T-CELs. NCMs are applicable to the computation of highly non-linear hyper-lines. This is possible through a relatively sophisticated use of the information available in the already computed points of the line. If a converged point of a T-CEL, i.e., an already computed T-CEP, is available, then, a NCMs can be started off to reliably compute the whole T-CEL, thus minimizing the need for user intervention. The availability of a fast and reliable method for computing T-CELs, makes possible to compute them, fast enough, in the whole domain available to the thermodynamic model chosen for representing the fluid phase equilibria of the system under study. Such domain includes temperatures as close to the absolute zero as desired, pressures as high (or as low) as desired, and extremely low concentrations. Computations at extreme conditions have the potential of unveiling new topologies, of possible existence in real systems, for T-CELs.

We also consider in this work the problem of detecting the key points where T-CELs originate or terminate. We use a model of the equation of state (EOS) type in wide ranges of conditions. The scope of this work is the phase equilibria that involves only fluid phases (solid phases are not considered in this work). Our goal is the characterization of a given combination of a model and parameters values from the point of view of the corresponding T-CELs.

Finally, in previous works, the naming of the different thermodynamic objects, such as the terminal points of T-CELs, is often confusing. In this work, we have defined a naming system for ternary systems which seems to be more clear than the previous ones.

2. Types of critical end lines

In this work we classify the T-CELs by considering how they originate and terminate. In general, the T-CELs originate at invariant points of the ternary system or at invariant points of a binary subsystem. On the other hand, T-CELs may terminate at invariant points or may have an indefinite end. The types of invariant points related to T-CELs are the following:

(i) Binary critical end point (B-CEP): in a B-CEP a binary critical phase is at equilibrium with a binary non-critical phase. A B-CEP sets the end of a binary liquid–liquid–vapor equilibrium line, where two of the fluid phases become critical [1].
(ii) Ternary critical end point of a four-phase equilibrium line (T-CEP-4PL): in a T-CEP-4PL a ternary critical phase is at equilibrium with two ternary non-critical phases. A T-CEP-4PL sets the end of a ternary liquid–liquid–liquid–vapor equilibrium line. At such end two of the fluid phases become critical. Although the acronym T-CEP-4PL refers to an end point of a four-phase equilibrium line, a T-CEP-4PL is also an end point of a T-CEL, i.e., a point where a system made of a critical phase and a non-critical phase becomes globally unstable (appearance of a third phase which is non-critical).
(iii) Ternary tricritical end point (T-TCEP): in a T-TCEP three phases at equilibrium become critical simultaneously. When a T-TCEP exists, an infinite number of paths within a ternary three-phase equilibrium hyper-surface, all leading to the T-TCEP, exist. However not every path within a ternary three-phase equilibrium hyper-surface contains a T-TCEP. Along a T-CEL (which as previously stated connects T-CEPs where a critical phase is at equilibrium with a non-critical phase), a T-TCEP is reached when the non-critical phase becomes critical with the critical phase.

The description of algorithms for computing the previously listed types of (invariant) end points of T-CELs is beyond the scope of this paper.

In this work we have identified ten different types of T-CELs based on how they originate and terminate. This is shown in Table 1. For instance a type 1 T-CEL (3rd row of Table 1) originates at a B-CEP of a binary subsystem of the ternary system and extends indefinitely either toward high pressures or toward low temperatures and pressures. We have computed T-CELs of this type in the present

Table 1
Types of ternary critical end lines.

Type	Originates at	Terminates at	Computed in this work?	Example shown in this work	Found in the literature?
1	B-CEP	High *P*, or low *T* and low *P*	Yes	T-CEL in Fig. B.6	No
2	B-CEP	B-CEP	Yes	T-CEL in Fig. 7	No
3	B-CEP	T-CEP-4PL	Yes	T-CEL(g),	Refs [3] and [25]
4	T-CEP-4PL	High P, or low T and low P	Yes	T-CEL(c,d,e), Figs. 1 and 4–6	No
5	T-CEP-4PL	T-CEP-4PL	Yes	T-CEL(f), Figs. 1 and 4–6	No
6	T-CEP-4PL	T-TCEP	Yes	T-CEL(a,b,h,i), Figs. 1–6, B.1 and B.2	Ref [3]
7	T-TCEP	T-TCEP	No	Not applicable	Possibly in ref [3]
8	B-CEP	T-TCEP	Yes	T-CEL(i), Figures B. 3–5	Ref [7]
9	Closed Loop	Closed Loop	No	Not applicable	Ref [26]
10	T-TCEP	Indefinite end	Yes	No	No

work, but have not found them in the literature. In type 2 T-CELs both B-CEPs could correspond to different binary subsystems of the ternary system, or to the same binary subsystem. T-CELs of type 7, where both T-TCEPs are different, seem to have been sketched by Adrian et al. [3]. The 5th column in Table 1 indicates figures which show examples of T-CELs of the types listed in Table 1. Notice that "type" and "topology" are not synonyms in this work, e.g., a T-CEL of certain type might have a monotonic pressure-temperature projection, while another T-CEL of the same type might show relative minima or maxima in its pressure-temperature projection.

3. Calculation of ternary critical end points

At a critical end point a critical phase is at equilibrium with a non critical phase. There are different ways of writing the system of equations that describes a critical phase. In this work we have used the criticality system of equations proposed by Michelsen [17]. For computing a T-CEP it is necessary to add, to the critical conditions, the isofugacity conditions between the critical and non-critical phases, together with the condition of uniformity of pressure and temperature throughout the heterogeneous system.

The resulting T-CEP system of equations, as it was implemented in this work, has 14 equations an 15 variables. The variables are the following:

$$T\ P\ V\ v^0\ V_x\ z_1\ z_2\ z_2\ z_3\ x_1\ x_2\ x_3\ u_1\ u_2\ u_3 \text{ and } \lambda$$

where T is the absolute temperature, P is the absolute pressure, v^0 is the molar volume of the critical phase, and V is certain total volume involved in the implementation of the criticality conditions. V_x is the molar volume of the non-critical phase. z_1, z_2 and z_3 are respectively the mole fractions of components 1, 2 and 3 in the critical phase. x_1, x_2 and x_3 have an analogous meaning but for the non-critical phase. u_1, u_2 and u_3 are the components of certain eigenvector appearing in the critical conditions proposed by Michelsen [17]. λ is the eigenvalue associated to the mentioned eigenvector. Notice that a T-CEP has a single degree of freedom. This is because the number of variables exceeds by one the number of equations in the T-CEP system of equations. In this work we solve all equations of the T-CEP system of equations simultaneously, using the Newton-Raphson method. This requires proper initial estimates, as discussed later in this paper. We provide the detailed description of the T-CEP system of equations in Appendix A. Notice that the way of implementing the system of variables and equations in Appendix A differs from that of Cismondi and Michelsen [18], which did not consider the eigenvalue and eigenvector components as explicit variables of the system.

4. Calculation of complete Ternary Critical end Lines

To start off the computation of a T-CEL we need to have available an already converged T-CEP. If the T-CEL originates at a B-CEP of, say, components 1 and 2, then, a T-CEP is calculated where component 3 is infinitely diluted (inf-T-CEP). All variables of the converged inf-T-CEP will have values identical to those of the B-CEP [18], except for the mole fractions of component 3 in both phases (z_3 and x_3), since z_3 and x_3 are variables that do not exist at the B-CEP. For converging the inf-T-CEP we set, as initial values, $z_3 = 10^{-4} \min(z_1, z_2)$ and $x_3 = 10^{-4} \min(x_1, x_2)$.

At a converged T-CEP-4PL a critical phase is at equilibrium with two non-critical phases. Therefore, a known T-CEP-4PL has information on two solutions to the T-CEP system of equations (Appendix A.1). One of them corresponds to the critical phase and one of the non-critical phases, while the other to the same critical phase and the remaining non-critical phase. It is thus clear that two different T-CELs meet at a T-CEP-4PL. In conclusion, a converged T-CEP-4PL provides two converged T-CEPs from which it is possible to start off the building of two complete T-CELs

We have not yet developed an algorithm to start off the building of a T-CEL from a known T-TCEP. Later in this paper we describe how we dealt with T-CELs containing T-TCEPs.

In this work, once we have available a converged ternary critical end point (T-CEP), obtained through Newton-Raphson iteration, we start the building of a complete T-CEL by resorting to a numerical continuation method (NCM) [19]. The computation of the next point of the T-CEL requires good initial estimates of the variables. The NCM used in this work assumes that the T-CEL has, locally, a linear behavior, in order to predict the next point from the information in the converged point. The NCM also identifies the optimum variable that should be specified for computing the next point of the T-CEL. This means that, e.g., a T-CEP could be obtained at a set temperature, and the next T-CEP in the T-CEL at a set pressure. This capability makes it possible to compute highly non-linear T-CELs, in a single run, with no convergence problems at potentially problematic points such as the so-called turning points where a variable of the T-CEL has a local extremum. The information needed both, to identify the optimum variable to be specified for computing the next point, and to set initial values for the variables of such next point, is contained within the Jacobian matrix of the function vector of the T-CEP system of equations (Appendix A.1), evaluated at the converged (previous) point. The basic features of the NCM used in this work are the same than those of the one used by Cismondi and Michelsen [18]. See Appendix A, section A.2, for more details on the NCM used in this work.

During the computation of a T-CEL, we monitor the behavior of the converged points. The following are the possible situations:

(a) If, along the T-CEL, the difference between the molar volumes of both phases tend to zero, and simultaneously the difference between the composition of the two phases also tends to zero, then, a T-TCEP is reached. This is one of the possible end points of a T-CEL.
(b) If, along the T-CEL, the concentration of one of the components of the ternary mixture tends to zero, for both equilibrium phases, then, a B-CEP has been reached.

(c) If the phases at equilibrium in a point of the T-CEL become globally unstable, being the previous computed T-CEPs globally stable, then, a T-CEP-4PL has been reached.
(d) If, while computing a T-CEL, none of the previous conditions (a,b,c) is met, and, either the pressure exceeds a preset high enough value, or the temperature becomes less than a preset low enough value, then, the calculation of the T-CEL is stopped. Notice that if any condition, among conditions (a), (b) and (c), is met, then, the computation of the T-CEL is also terminated.

The stability test that we used to monitor the existence of T-CEPs-4PL is a standard stability test [20]. For performing it, for a given converged T-CEP, we searched for local minima of the tangent plane distance (tpd) function within the space of (ternary) composition of the trial phase. A negative tpd is indicative of a globally unstable T-CEP.

5. Results and discussion

In this work we computed T-CELs of different types for the ternary systems *ethane + propane + n-eicosane* (system "I") and *carbon dioxide + water + 2-propanol* (system "II"). These systems have been chosen in this work, on one hand, because of the availability of experimental T-CEL patterns for both of them ([7] [3]). On the other hand, systems "I" and "II" differ in the source of non-ideality: system "I" is made of non-polar components, while system "II" contains two highly polar components (water and 2-propanol) capable of forming hydrogen bonds. Non idealities are given in system "I" by differences in molecular size while, in system "II", non idealities are mainly due to differences in energetic interactions. System "I" is known to have a relatively simple experimental phase equilibrium behavior [7]. In contrast, system "II" has a highly complex experimental behavior, which includes four-phase equilibria, as shown on page 188 of ref [3]. The computation of T-CELs for system "I" would be a relatively straightforward test for the proposed algorithm, and the calculation of T-CELs for system "II" would be a more stringent test.

For the computation of T-CELs, we used the Soave-Redlich-Kwong equation of state (SRK-EOS) [10] coupled to quadratic mixing rules. The SRK-EOS is one of the best known modifications of the van der Waals EOS. We have chosen the SRK-EOS for this study because it has been previously applied to ternary systems that show a complex phase behavior [9], and because it is representative of a family of well-established models regularly used in engineering computations. However, the reader should be aware of the fact that the SRK-EOS, and other models of the equation of state type, may be affected by some numerical pitfalls [21,22]. The values for the interaction parameters used in the calculations are given in Table 2 together with the predicted type of phase behavior for the binary systems [1]. We obtained this last information using the algorithms proposed in reference [18]. Although the parameters from ref [5] shown in Table 2 were used in ref [5] with the Peng-Robinson EOS, in this work we used such parameters with the SRK-EOS. Notice that the focus of this work is the computation of T-CELs rather than the reproduction of experimental information. We obtained the pure compound critical temperatures and pressures, and acentric factors, from de the DIPPR database [23]. Figs. 1–7 show the computed pressure temperature projections of the univariant lines of these ternary systems. Additional results are shown in Appendix B.

Fig. 1 presents several T-CELs calculated in this work for the system *carbon dioxide + water + 2-propanol* over wide ranges of temperature and pressure, using the model and parameter values indicated in Table 2. We identify such lines as "a", "b", "c", etcetera. We observe in Fig. 1 several types of CELs, among those listed in

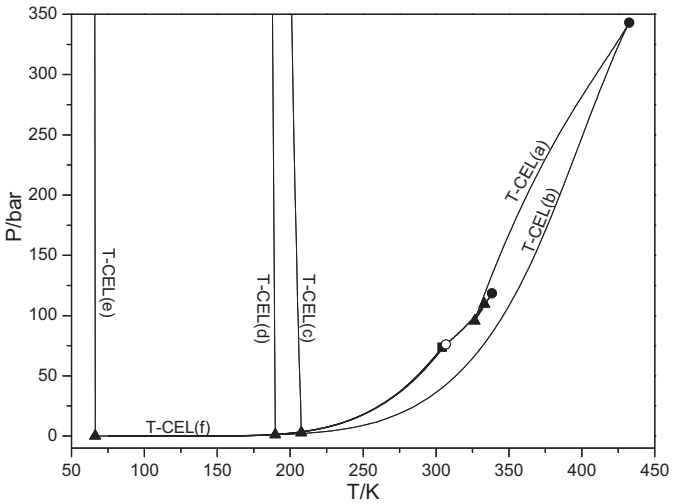

Fig. 1. Calculated Pressure–Temperature projection of univariant lines of the system Carbon Dioxide + Water + 2-Propanol. Square: Critical point of pure CO_2. Empty Circle: Binary critical end point of the sub-system $CO_2 + H_2O$ (Type III). Triangle: Ternary critical end point of a four phase line (T-CEP-4PL). Full Circle: Ternary tricritical end point (T-TCEP). The letters (a)-(f) are used to distinguish between the various T-CELs discussed in the text.

Table 1. T-CEL(e) originates at low-temperature low-pressure T-CEP-4PL, and extends to high pressures. T-CELs (c) and (d) originate also at T-CEPs-4PL of intermediate temperature. These lines are globally stable within the universe of the model, where only the fluid state exists. This work does not consider the existence of the solid state. The pure compound melting temperatures for the system of Fig. 1 are the following [23]: carbon dioxide: 216.6 K, water: 273.1 K, and 2-propanol: 185.3 K. Thus, the T-CELs of lower temperature shown in Fig. 1 should be metastable with respect to equilibria involving solid phases.

Fig. 2 shows, among other T-CELs, the line T-CEL(g). We computed it starting from a B-CEP, i.e., from the binary *carbon dioxide + water* critical end point (empty circle). The T-CEL(g) ends at a T-CEP-4PL. The behavior of the pressure-temperature projection of the T-CEL(g) is quite linear. That is not necessarily the case for

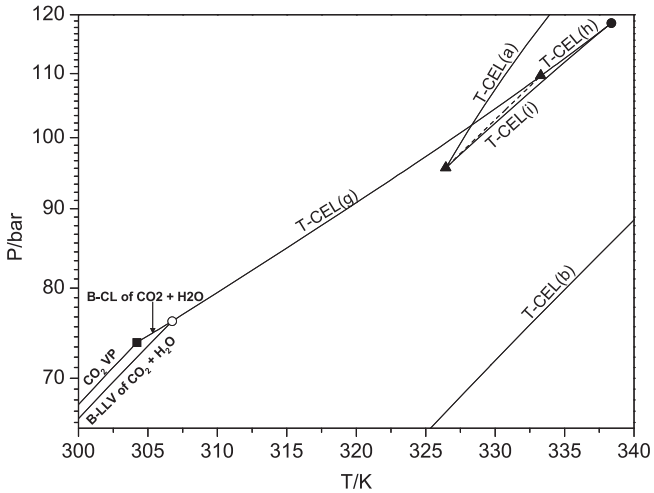

Fig. 2. Zoom Fig. 1. Calculated Pressure–Temperature projection of univariant lines of the system Carbon Dioxide + Water + 2-Propanol. Square: Critical point of pure CO_2. Empty Circle: Binary critical end point (B-CEP). Triangle: Ternary critical end point of a four phase line (T-CEP-4PL). Full Circle: Ternary tricritical end point (T-TCEP). Dashed Line: Ternary four-phase equilibrium line. B-LLV means "binary liquid–liquid–vapor equilibrium line". VP means "pure compound vapor–liquid equilibrium line". B-CL means "binary critical line". The letters (a), (b), (g), (h) and (i) are used to distinguish between the various T-CELs discussed in the text.

Table 2
Interaction parameters used with the SRK-EOS [10].

Binary system	Attractive interaction parameter (k_{ij})	Repulsive interaction parameter (l_{ij})	Reference	SRK Predicted type of phase behavior [1]
$CO_2 + H_2O$	−0.053	0.0	[5]	III
CO_2 + 2-Propanol	0.017	0.0	[5]	II
H_2O + 2-Propanol	−0.207	0.0	[5]	I
Ethane + Propane	0.0616	0.0916	[7]	I
Ethane + n-Eicosane	0.0263	0.0189	[7]	IV
Propane + n-Eicosane	0.0114	0.0086	[7]	II

other projections, e.g., the pressure-molar volume projection (see Fig. B.5), or the T-CEL pressure-temperature projection of other systems (see Fig. 7).

In Fig. 3 we see the lines T-CEL(h) and T-CEL(i), The T-CEL(h) connects a T-CEP-4PL (triangle) with a T-TCEP (full circle). The computation of the T-CEL(h) started off at its T-CEP-4PL and ended when the non-critical phase became identical (i.e., critical) to the critical phase, which indicated the existence of the T-TCEP. Since we have not yet developed an algorithm for computing a T-CEL starting the calculation off at a T-TCEP, we computed the line T-CEL(i) as follows. We first computed a four-phase equilibrium point. Next we computed the whole four-phase line until we found the T-CEP-4PL of lowest temperature in Fig. 3. We finally used such point to start off the computation of the line T-CEL(i). Notice that the description of the algorithm for calculating four-phase lines is beyond the scope of this paper. Guidelines for multiphase equilibrium calculations are given, e.g., in sections 3.1 and 3.2 of ref [3]. In Fig. 3 several T-CELs are concentrated within relatively narrow ranges of pressure and temperature. Besides, in the pressure-temperature projection shown in Fig. 3, there is an intersection point between the T-CEL(g) and the TCEL(a). These features could lead to unwanted jumps from one T-CEL to another while building a T-CEL. The chance of occurrence of such jumps is minimized by the use of NCMs, as the one implemented in this work.

From the T-CEP-4PL (triangle) of lowest temperature in Fig. 3, we started off the computation of the line T-CEL(a), which ends at the T-TCEP of maximum temperature and maximum pressure in Fig. 1. From such T-TCEP a second T-CEL originates, i.e., the line T-CEL(b) (see Fig. 1), which as the line T-CEL(i) (see Fig. 3), could not be computed starting off at its T-TCEP. In the case of T-CEL(b) line, we computed first a ternary three-phase equilibrium line at constant pressure starting from an already converged binary *carbon dioxide + water* three-phase equilibrium [18] point (Fig. 2). The calculation of the ternary three-phase line was terminated when two of the phases became critical, i.e., at a point of the line T-CEL(b), i.e., at a T-CEP. From this point the whole line T-CEL(b) was built using the NCM. This was done in two stages. One of them covered the range from the found T-CEP to the T-TCEP of T-CEL(b). The second stage covered the range from the found T-CEP to the other end point of T-CEL(b) which was found to be a T-CEP-4PL (lowest temperature triangle in Fig. 4). The procedure for calculating the ternary three-phase line can be applied for instance at 70 bar (see Fig. 2). The description of the algorithm for computing ternary three-phase equilibrium lines is beyond the scope of this paper (the reader may wish to consult ref [3], where a quite detailed account on how to calculate multiphase equilibria is provided). Fig. 4 shows, among others, a couple of calculated T-CELs [T-CEL(c) and T-CEL(d)] that originate at corresponding low-pressure T-CEPs-4PL (Fig. 5). Notice the logarithmic scale for the pressure in Fig. 4. The narrow temperature and pressure ranges of Fig. 5 makes it possible to visualize that the line T-CEL(f) originates at the same T-CEP-4PL than the line T-CEL(c). Fig. 6 shows that the other end point of the line T-CEL(f) is also a T-CEP-4PL of very low temperature and extremely low pressure. The lines T-CEL(c), (d), (e) and (f) were all calculated starting off from a suitable T-CEP-4PL.

Notice in Fig. 6 that from the T-CEP-4PL that connects the lines T-CEL(e) and T-CEL(f) another ternary four-phase equilibrium line originates, which is not shown in Fig. 6. Such line ends at another (not shown) T-CEP-4PL. We should also note that the calculated univariant lines [18] of the binary sub-systems *carbon dioxide + 2-propanol* and *water + 2-Propanol* are not shown in this work. Besides,

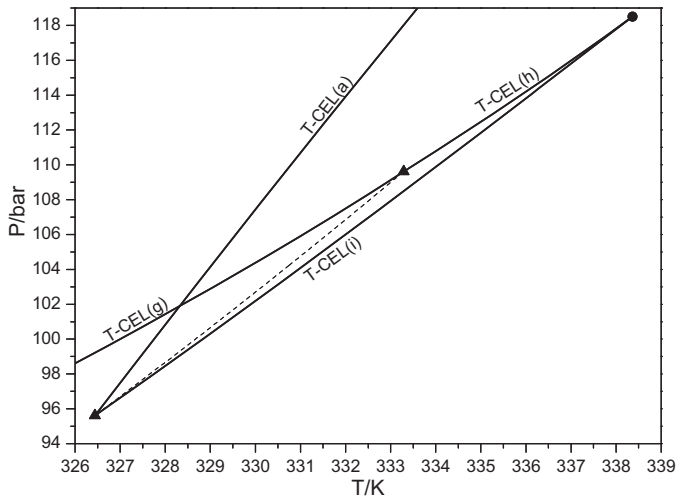

Fig. 3. Zoom Fig. 2. Calculated Pressure–Temperature projection of univariant lines of the system Carbon Dioxide + Water + 2-Propanol. Triangles: Ternary critical end point of a four phase line (T-CEP-4PL). Full Circle: Ternary tricritical end point (T-TCEP). Dashed Line: Ternary four-phase equilibrium line. The letters (a), (g), (h) and (i) are used to distinguish between the various T-CELs discussed in the text.

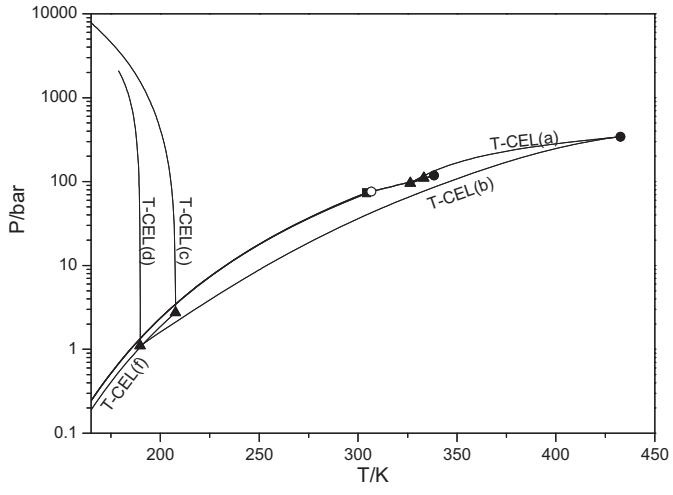

Fig. 4. Calculated Pressure–Temperature projection of univariant lines of the system Carbon Dioxide + Water + 2-Propanol. Square: Critical point of pure CO_2. Empty Circle: Binary critical end point of the sub-system $CO_2 + H_2O$ (Type III). Triangles: Ternary critical end point of a four phase line (T-CEP-4PL). Full Circle: Ternary tricritical end point (T-TCEP). The letters (a)–(d) and (f) are used to distinguish between the various T-CELs discussed in the text.

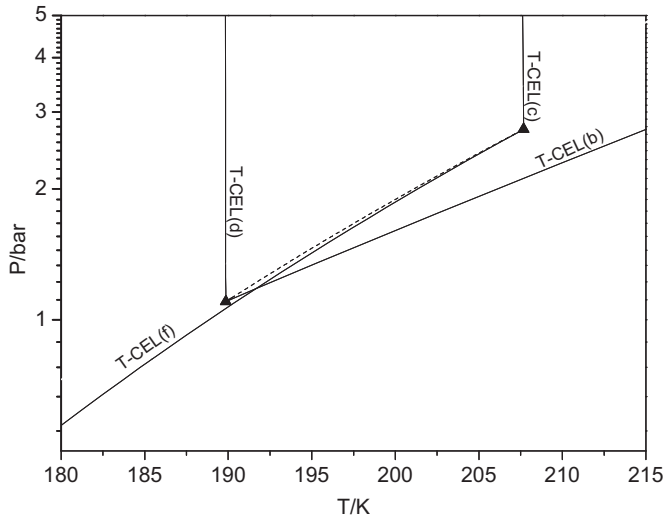

Fig. 5. Zoom of Fig. 4. Calculated Pressure–Temperature projection of univariant lines of the system Carbon Dioxide + Water + 2-Propanol. Triangles: Ternary critical end point of a four phase line (T-CEP-4PL). Dashed Line: Ternary four-phase equilibrium line. The letters (b), (c), (d) and (f) are used to distinguish between the various T-CELs discussed in the text.

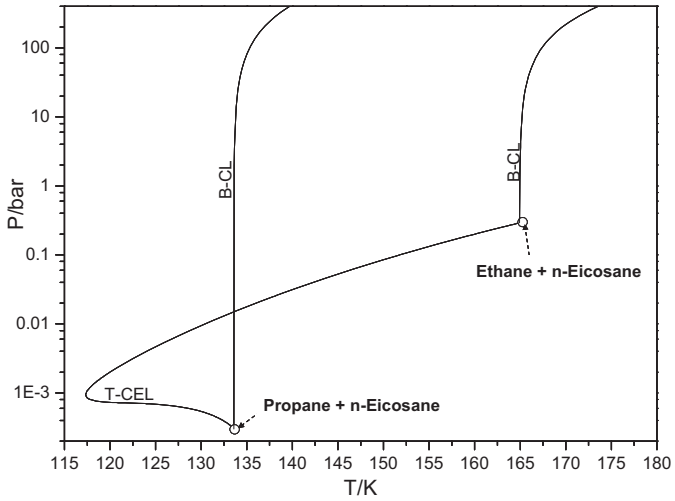

Fig. 7. Calculated Pressure–Temperature projection of univariant lines of the system Ethane + Propane + n-Eicosane. Empty circle: Binary critical end point (B-CEP). B-CL: binary critical line.

only some calculated univariant lines [18] are shown for the binary sub-system *carbon dioxide + water* (see Fig. 2). Appendix B shows additional projections both, for the system *carbon dioxide + water* and for the system *carbon dioxide + water + 2-propanol* (Figs. B.1 and B.2).

Fig. 7 shows, for the system Ethane + Propane + n-Eicosane, a calculated T-CEL that connects a B-CEP of the sub-system ethane + n-eicosane with a B-CEP of the sub-system propane + n-eicosane. Both B-CEPs are end points of corresponding binary critical lines which are of the liquid–liquid type, and are also shown in Fig. 7. The binary lines in Fig. 7 were calculated according to reference [18]. It is clear that the T-CEL of Fig. 7 has a highly non-linear behavior: it presents a turning point, i.e., a local minimum temperature in this case (at about 117 K). NCMs as the one used in this work are specially suited for dealing with turning points. Appendix B shows additional T-CELs for this system (Ethane + Propane + n-Eicosane, Figs. 3–5)

Notice that this work deals with calculation algorithms, i.e., with the calculation of T-CELs, for a specified fluid state model, and for specified parameter values for the ternary system of interest. The fluid state is the only state available to the SRK-EOS model, i.e., the model does not account for the possible appearance of solid phases. The melting points of the components of the ternary system of Fig. 7 are the following [23]: ethane: 90.4 K, propane: 85.5 K and n-eicosane: 309.6 K. The maximum temperature in Fig. 7 is about 175 K which is much lower than 309.6 K. Therefore, the lines in Fig. 7 would be metastable with respect to equilibria involving solid phases.

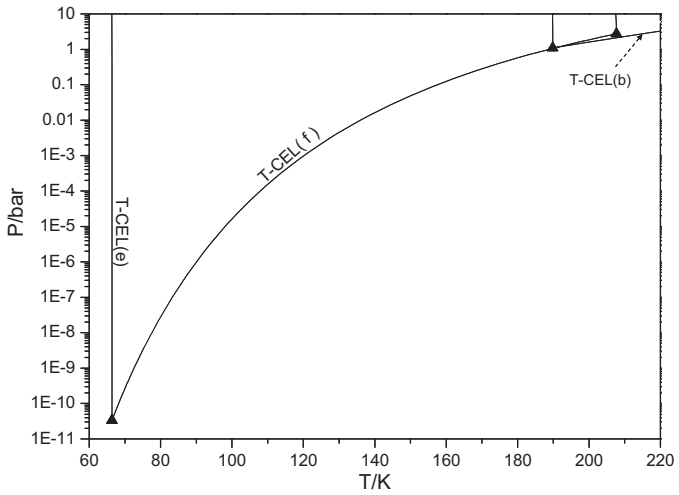

Fig. 6. Zoom of Fig. 1. Calculated Pressure–Temperature projection of univariant lines of the system Carbon Dioxide + Water + 2-Propanol. Triangles: Ternary critical end point of a four phase line (T-CEP-4PL). The letters (b), (e) and (f) are used to distinguish between the various T-CELs discussed in the text.

6. Remarks and conclusions

Since ternary critical end lines (T-CELs) are boundaries for the three phase equilibria of ternary systems, it is important to have robust algorithms available for computing T-CELs for a given ternary system, given model and given model parameter values.

Due to the confusing terminology used previously, in the literature, regarding a number of ternary phase equilibrium univariant lines and invariant points, we have defined in this work a new naming system that seems to be free from ambiguity. This naming system led to acronyms such as T-CEL, T-TCEP and T-CEP-4PL.

We have applied a numerical continuation method (NCM) to the calculation of T-CELs over wide ranges of conditions. We have also proposed systematic ways to start off the computation of the T-CELs. The NCM did not experience unwanted jumps between different T-CELs and showed to be robust in the presence of turning points (e.g., Fig. 7). A key feature of our calculation algorithm was the use of a logarithmic scaling (see Appendix A.1) for the (positive) variables of the T-CEP system of equations. This made possible to explore the behavior of the ternary systems at extreme conditions, as, e.g., the extremely low pressures in part of Fig. 6.

The characterization of T-CELs carried out in this work within much wider ranges of conditions than in previous works, reveal that, within the universe of the fluid-state model, there can be, for a ternary system, a large number of T-CELs whose interconnection may be highly complex, as shown, e.g., in Fig. 1.

With regard to the types of T-CELs, we have summarized them in Table 1. We believe that this table is quite comprehensive. However, Table 1 is limited to the types of T-CELs that we have observed, either in this work or in the literature, or both. The T-CEL topologies found in this work are more complex than those considered in ref [16], in which a classification for the fluid phase behavior of ternary systems was proposed. In this work, we have shown computed

T-CELs of types 1, 2, 3, 4, 5, 6 and 8 (see Table 1). We have also found a computed T-CEL originating at a T-TCEP and extending indefinitely to high pressure (type 10 in Table 1). We have not yet found, in our calculations, T-CELs of type 7. Finally, T-CELs of types not considered in Table 1 might exist for the SRK-EOS, when coupled to combinations of pure compound and interaction parameter values not considered in this work. Besides, types of T-CELs not listed in Table 1 might exist for equations of state different from the SRK-EOS.

Our calculations suggest the possibility of T-CEL topologies not previously reported in the literature. Since the thermodynamic model (SRK-EOS) that generated such topologies is a relatively simple one, our conjecture is that some of the new topologies might be observed experimentally in the future. This conjecture should be handled with care. The reasons are the following: (a) some of our calculated T-CELs should be (at least partially) metastable with respect to equilibria involving solid phases. (b) complex enough thermodynamic models may generate behaviors not seen in real systems [21,22].

Among our future goals is to completely automate the generation of diagrams as the one in Fig. 1.

Acknowledgements

We are grateful, for their financial support, to the following institutions: Consejo Nacional de Investigaciones Científicas y Técnicas de la República Argentina (CONICET), Universidad Nacional del Sur (U.N.S., Arg.), Agencia Nacional de Promoción Científica y Tecnológica (ANPCyT, Arg.) Capes/Brazil, Fundação Araucária (Brazil), FAPESP (Brazil) and CNPq (Brazil). M.S.Z. was a CAPES/BRASIL Grantee at State University of Maringá during part of year 2013.

Appendix A. System of Equations for the ternary critical end point calculation

A.1. System of Equations for the ternary critical end point calculation

The system of equations that has to be solved for computing a ternary critical end point (T-CEP) is the following:

$$F = \begin{bmatrix} F_1 \\ F_2 \\ F_3 \\ F_4 \\ F_5 \\ F_6 \\ F_7 \\ F_8 \\ F_9 \\ F_{10} \\ F_{11} \\ F_{12} \\ F_{13} \\ F_{14} \end{bmatrix} = \begin{bmatrix} \det(\mathrm{M}^* - \lambda I) \\ (M^*_{11} - \lambda)u_1 + M^*_{12}u_2 + M^*_{13}u_3 \\ M^*_{21}u_1 + (M^*_{22} - \lambda)u_2 + M^*_{23}u_3 \\ u_1^2 + u_2^2 + u_3^2 - 1 \\ \left(\frac{\partial^2 tpd^*}{\partial s^2}\right)_{s=0} \\ \left(\frac{\partial^3 tpd^*}{\partial s^3}\right)_{s=0} \\ V - v^0 \\ \ln \hat{f}_1(T, V_x, \mathrm{x}) - \ln \hat{f}_1(T, v^0, \mathrm{z}) \\ \ln \hat{f}_2(T, V_x, \mathrm{x}) - \ln \hat{f}_2(T, v^0, \mathrm{z}) \\ \ln \hat{f}_3(T, V_x, \mathrm{x}) - \ln \hat{f}_3(T, v^0, \mathrm{z}) \\ P - \psi(T, v^0, \mathrm{z}) \\ P - \psi(T, V_x, \mathrm{x}) \\ z_1 + z_2 + z_3 - 1 \\ x_1 + x_2 + x_3 - 1 \end{bmatrix} = 0 \qquad (1)$$

In system (1), T is the absolute temperature and P is the absolute pressure. $\hat{f}_i$ is the function of temperature, total volume, and numbers of moles of the components in the multicomponent mixture (n_i, i = from 1 to number of components) that explicitly connects such variables with the fugacity of component "i" in the mixture. The chosen equation of state (SRK-EOS in this work) imposes the form of function $\hat{f}_i$.

In system (1), the first equation, i.e., the equation $F_1 = 0$, is the equation for calculating the eigenvalues of matrix $\mathbf{M}^*$. I is the identity matrix and λ is the eigenvalue of matrix $\mathbf{M}^*$ of minimum absolute value. The elements of matrix $\mathbf{M}^*$ are defined as follows:

$$M^*_{ij} = \sqrt{z_i z_j}\left[\left(\frac{\partial \ln \hat{f}_i}{\partial n_j}\right)_{T,V,n_m}\right]_{T,V,z} \quad \text{with } m = 1 \text{ to } 3 \text{ subject to } m \neq j \qquad (2)$$

In the expression resulting from the differentiation process in Eq. (2), vector $\boldsymbol{n}$ (whose elements are the numbers of moles of the components) has to be replaced by vector $\mathbf{z}$ (whose elements are the mole fractions of the components in the critical phase).

In equations $F_2 = 0$, $F_3 = 0$, and $F_4 = 0$, in system (1), u_1, u_2 and u_3 are the components of the (normalized) eigenvector of matrix $\mathbf{M}^*$, associated to eigenvalue λ. $F_2 = 0$ and $F_3 = 0$ correspond to the standard equations for computing the eigenvectors. $F_4 = 0$ is a normalization equation that imposes a unity module for eigenvector $\mathbf{u}$.

In eqs $F_5 = 0$ and $F_6 = 0$, tpd^* is defined as follows:

$$tpd^* = [tpd(T, V, \mathbf{n})]_{T,V,n_i = n_i^*} \qquad (3)$$

where tpd is the tangent plane distance function, defined as follows:

$$tpd(T, V, \mathbf{n}) = \sum_i n_i[\ln \hat{f}_i(T, V, \mathbf{n}) - \ln \hat{f}_i(T, v^0, \mathbf{z})] - \frac{V}{RT}(\psi(T, V, \mathbf{n}) - (\psi(T, v^0, \mathbf{z})) \qquad (4)$$

R is the universal gas constant. Function ψ connects the total volume, the vector n, and the absolute temperature to the absolute pressure. Function ψ is in this work the pressure-explicit SRK-EOS coupled to quadratic mixing rules. In Eq. (4) v^0 is the molar volume of the critical phase and $\mathbf{z}$ is a vector with elements z_1, z_2 and z_3 which are respectively the mole fractions of components 1, 2 and 3 in the critical phase. According to Eq. (3), the components of vector $\mathbf{n}$ have to be set, within Eq. (4), as follows:

$$n_i^* = z_i + s u_i \sqrt{z_i} \qquad (5)$$

where variable "s" is a distance parameter. From eqs (3) and (4), it should be clear that tpd^* is a function of T, V, $\mathbf{z}$, $\mathbf{u}$, v^0 and s. The dependence of tpd^* on variable "s" makes it possible to obtain the analytical expressions for the partial derivatives of tpd^*, which are required by eqs $F_5 = 0$ and $F_6 = 0$ in system (1). Such equations prescribe that the partial derivatives have to be evaluated at $s = 0$. For this reason, "s" is not a variable of the system of equations (1).

Notice that eq $F_7 = 0$ in system (1) imposes the equality between variables V *and* v^0. Equations $F_8 = 0$, $F_9 = 0$ and $F_{10} = 0$ in system (1) impose the isofugacity condition of the components of the ternary system in the critical and noncritical phases. $\hat{f}_i(T, V_x, \mathbf{x})$ is the fugacity of the ith component in the non-critical phase and $\hat{f}_i(T, v^0, \mathbf{z})$ is the fugacity of the ith component in the critical phase. $\boldsymbol{x}$ is the mole fraction vector, and V_x the molar volume, both for the non-critical phase.

Eqs $F_{11} = 0$ and $F_{12} = 0$ in system (1) establish that the pressure is the same for the critical and non-critical phases. Eq $F_{11} = 0$ corresponds to the critical phase and eq $F_{12} = 0$ to the non-critical phase. Finally, eqs $F_{13} = 0$ and $F_{14} = 0$ impose that the mole fractions, in a given phase, must add up to unity.

The T-CEP system of equations [system (1)] has 14 equations and 15 variables. The list of variables is summarized as follows:

$$T\ P\ V\ v^0\ V_x\ z_1\ z_2\ z_3\ x_1\ x_2\ x_3\ u_1\ u_2\ u_3 \text{ and } \lambda$$

Since the number of variables exceeds by one the number of equations, system (1) has a degree of freedom and therefore defines a hyper-line in a 15D space.

Function *tpd* in Eq. (4), is a difference, i.e., the Helmholtz energy at (T, V, $\mathbf{n}$) minus the linear approximation to the Helmholtz energy at (T, v^0, $\mathbf{z}$), evaluated, such approximation, also at (T, V, $\mathbf{n}$). In other words, the tangent plane distance function is the difference between the Helmholtz energy surface and the plane that is tangent to the surface at (T, v^0, $\mathbf{z}$), as a function of (T, V, $\mathbf{n}$).

In Eq. (4) the phase at (T, v^0, $\mathbf{z}$) is the tested phase and the phase at (T, V, $\mathbf{n}$) is the trial phase. A negative *tpd* value implies that the tested phase is not stable.

In system (1), eqs $F_1 = 0$ to $F_7 = 0$, $F_{11} = 0$ and $F_{13} = 0$ are the criticality conditions. They are essentially the same than those proposed by Michelsen [17]. The number (nine) of criticality conditions in this work comes from the fact that the variables involved are all considered explicitly. In this work the critical equations are solved simultaneously (and together with the equations that set the equilibrium between the critical and non-critical phases).

The actual calculations where performed in this work using logarithmically scaled variables. Only positive variables can be scaled according to the conventional recipe for logarithmic scaling. To rewrite system (1) in terms of scaled variables we proceed as follows. Consider for instance the temperature T. We define the scaled temperature T^* as follows:

$$T^* = \ln(T) \tag{5b}$$

In system (1) variable T has to be replaced by its expression in terms of T^*, as dictated by the following equation, derived from Eq. (5b):

$$T = \exp(T^*) \tag{5c}$$

System (1) thus becomes written in terms of the following variables:

$$T^*\ P^*\ V^*\ v^{0*}\ V_x^*\ z_1^*\ z_2^*\ z_3^*\ x_1^*\ x_2^*\ x_3^*\ u_1\ u_2\ u_3 \text{ and } \lambda$$

Variables u_1, u_2, u_3 and λ have not been scaled in this work, because they can be negative.

The important point is that the range of variation of logarithmically scaled variables is much narrower than that of non-scaled variables. This becomes extremely important when the mole fraction of a component tends to zero.

A.2. Numerical continuation method for computing complete T-CELs

To start the computation of a T-CEL we need a first converged point, i.e., a solution of system (1). As explained in the main text of this paper, in this work we have, almost always, chosen an end point of the T-CEL being built as first converged point. The initialization of a first point of a T-CEL is also explained in the main text. System (1) is solved using the Newton-Raphson method.

In what follows we explain how the T-CEL is built once a first converged point has already been obtained. We define vector Λ as the vector whose fifteen components are the variables of system (1). Thus:

$$\Lambda^{\mathrm{T}} = [T\ P\ V\ v^0\ V_x\ z_1\ z_2\ z_3\ x_1\ x_2\ x_3\ u_1\ u_2\ u_3\ \lambda] \tag{6}$$

Since system (1) has a degree of freedom we need to add a specification equation to system (1). In this way the number of variables become equal to the number of equations and a solution for system (1) can be searched for.

The required additional equation has the following general form:

$$\Lambda_s - S_{spec} = 0 \tag{7}$$

Equation (7) is the specification equation, where Λ_s is the specified variable and S_{spec} is the value assigned to the specified variable. For instance, if we want to compute a T-CEP at 100 bar, then, we set $\Lambda_s = P$ and $S_{spec} = 100$. Thus, in such a case, from Eq. (7), the specification equation becomes [$P - 100 = 0$].

We represent the 15×15 system of equations obtained by adding Eq. (7) to system (1) as follows:

$$F^{(15)} = 0 \tag{8}$$

The superscript $^{(15)}$ means that the vector function $F^{(15)}$ has 15 components. Notice that the last component of vector function $F^{(15)}$ is $F_{15} = \Lambda_s - S_{spec}$.

System (8) is solved using the Newton-Raphson multi-variable method. The solution to system (8) depends on S_{spec}. Thus all variables of vector Λ are functions of S_{spec}. The expressions for the derivatives of the variables in vector Λ with respect to S_{spec} are obtained through implicit differentiation of all equations of system (8) with respect to S_{spec}. This is represented by the following equation:

$$J_{F^{(15)}} \left(\frac{\mathrm{d}\Lambda}{\mathrm{d}S_{spec}} \right) + \left(\frac{\partial F^{(15)}}{\partial S_{spec}} \right) = 0 \tag{9}$$

where $J_{F^{(15)}}$ is the Jacobian matrix of vector function $F^{(15)}$ and $(\mathrm{d}\Lambda/\mathrm{d}S_{spec})$ is the sensitivity vector whose components are the following:

$$\frac{\mathrm{d}\Lambda}{\mathrm{d}S_{spec}} = \left[\begin{array}{cccccccccc} \frac{\mathrm{d}T}{\mathrm{d}S_{spec}} & \frac{\mathrm{d}P}{\mathrm{d}S_{spec}} & \frac{\mathrm{d}V}{\mathrm{d}S_{spec}} & \frac{\mathrm{d}v^0}{\mathrm{d}S_{spec}} & \frac{\mathrm{d}V_x}{\mathrm{d}S_{spec}} & \frac{\mathrm{d}z_1}{\mathrm{d}S_{spec}} & \frac{\mathrm{d}z_2}{\mathrm{d}S_{spec}} & \frac{\mathrm{d}z_3}{\mathrm{d}S_{spec}} \\ & \frac{\mathrm{d}x_1}{\mathrm{d}S_{spec}} & \frac{\mathrm{d}x_2}{\mathrm{d}S_{spec}} & \frac{\mathrm{d}x_3}{\mathrm{d}S_{spec}} & \frac{\mathrm{d}u_1}{\mathrm{d}S_{spec}} & \frac{\mathrm{d}u_2}{\mathrm{d}S_{spec}} & \frac{\mathrm{d}u_3}{\mathrm{d}S_{spec}} & \frac{\mathrm{d}\lambda}{\mathrm{d}S_{spec}} \end{array} \right]^T \tag{10}$$

Notice that only the last element of $F^{(15)}$ depends explicitly on S_{spec}. Also, it does it in a linear way (remember that $F_{15} = \Lambda_s - S_{spec}$). Thus, we write

$$\left(\frac{\partial F}{\partial S_{spec}} \right) = [0\,0\,0\,0\,0\,0\,0\,0\,0\,0\,0\,0\,0\,0\,-1]^{\mathrm{T}} \tag{11}$$

Notice that Eq. (9) is the result of applying the chain rule.

When a solution to system (8) is available, then, $J_{F^{(15)}}$ is evaluated and system (9) is solved for $(\mathrm{d}\Lambda/\mathrm{d}S_{spec})$. To fix ideas, the vector $(\mathrm{d}\Lambda/\mathrm{d}S_{spec})$ provides information on the rate of change of each of the variables of vector Λ with respect to parameter S_{spec}, while keeping Eq. (8) satisfied. In other words, $(\mathrm{d}\Lambda/\mathrm{d}S_{spec})$ tells how the variables of vector Λ change when parameter S_{spec} changes, when going from one T-CEP to another T-CEP that differs differentially from the first T-CEP.

The information contained in $(\mathrm{d}\Lambda/\mathrm{d}S_{spec})$ is used to predict, through linear extrapolation, the next point of the T-CEL to be calculated after changing the variable S_{spec} by an amount ΔS_{spec}. This is done as follows:

$$\Lambda^0_{next\ point} = \Lambda_{conv.point} + \left(\frac{\mathrm{d}\Lambda}{\mathrm{d}S_{spec}} \right)_{conv.point} \Delta S_{spec} \tag{12}$$

$\Lambda^0_{next\ point}$ is the initial estimate for vector Λ of the next point, of the T-CEL, to be computed. ΔS_{spec} is set by considering the number of iterations required to obtain the converged point. A small number of iterations justifies the increase in ΔS_{spec}, while a large number has the opposite effect.

Besides, vector $(\mathrm{d}\Lambda/\mathrm{d}S_{spec})$ is used to identify the variable to be specified for computing the next point of the T-CEL. Such variable corresponds to the element of vector $(\mathrm{d}\Lambda/\mathrm{d}S_{spec})$ with maximum

absolute value. A change in the specified variable means that variable Λ_s in Eq. (7) is changed by another one chosen among those in vector Λ, and that the value of S_{spec} is also changed in Eq. (7) so that it becomes consistent with the new nature of the specified variable. A change in the specified variable requires to recalculate the sensitivity vector by dividing all its components by the element of the original sensitivity vector with maximum absolute value. This recalculated vector is the one to be used for predicting, through Eq. (12), the next point of the T-CEL. Allowing changes in the specified variable is what makes possible to avoid wrong specifications at turning points, which would lead to lack of convergence.

To clarify the previous paragraph, we will use the concise subscript "cp" for "converged point" and the subscript "np" for "next point" of the T-CEL being computed. We identify the vector $(d\Lambda/dS_{spec})$, the variable Λ_s and the parameter S_{spec}, all of them at the "cp", as $(d\Lambda/dS_{spec})_{cp}$, $\Lambda_{s,cp}$, $S_{spec,cp}$. Assume that $\Lambda_{s,cp} = P$. This means that $S_{spec,cp}$ is the value of the system pressure that was specified to obtain the "cp". Also assume, with reference to Eq. (10), that the component of $(d\Lambda/dS_{spec})_{cp}$ with maximum absolute value is, e.g., the one involving the variable V_x, i.e., the scalar $(dV_x/dS_{spec})_{cp}$. This means that $\Lambda_{s,np} = V_x$ and that $S_{spec,np}$ will be the value of V_x specified to compute the "np". In this case, the sensitivity vector for the "cp" has to be recalculated as follows:

$$\left(\frac{d\Lambda}{dS_{spec}}\right)_{cp} \leftarrow \left(\frac{(d\Lambda/dS_{spec})_{cp}}{(dV_x/dS_{spec})_{cp}}\right) \tag{13}$$

Notice that the left hand side of assignment (13) corresponds to $\Lambda_{s,cp} = V_x$ and $S_{spec,cp}$ equal to the value of V_x of the "cp". To predict the "np", Eq. (12) is used, plugging in the recalculated sensitivity vector and setting ΔS_{spec} (which is equal to $[S_{spec,np} - S_{spec,cp}]$) equal to the difference between the desired value of V_x for the "np" and the value of V_x of the "cp".

Fig. A.2.1 presents a graphical flowchart corresponding to the described procedure for computing a T-CEL.

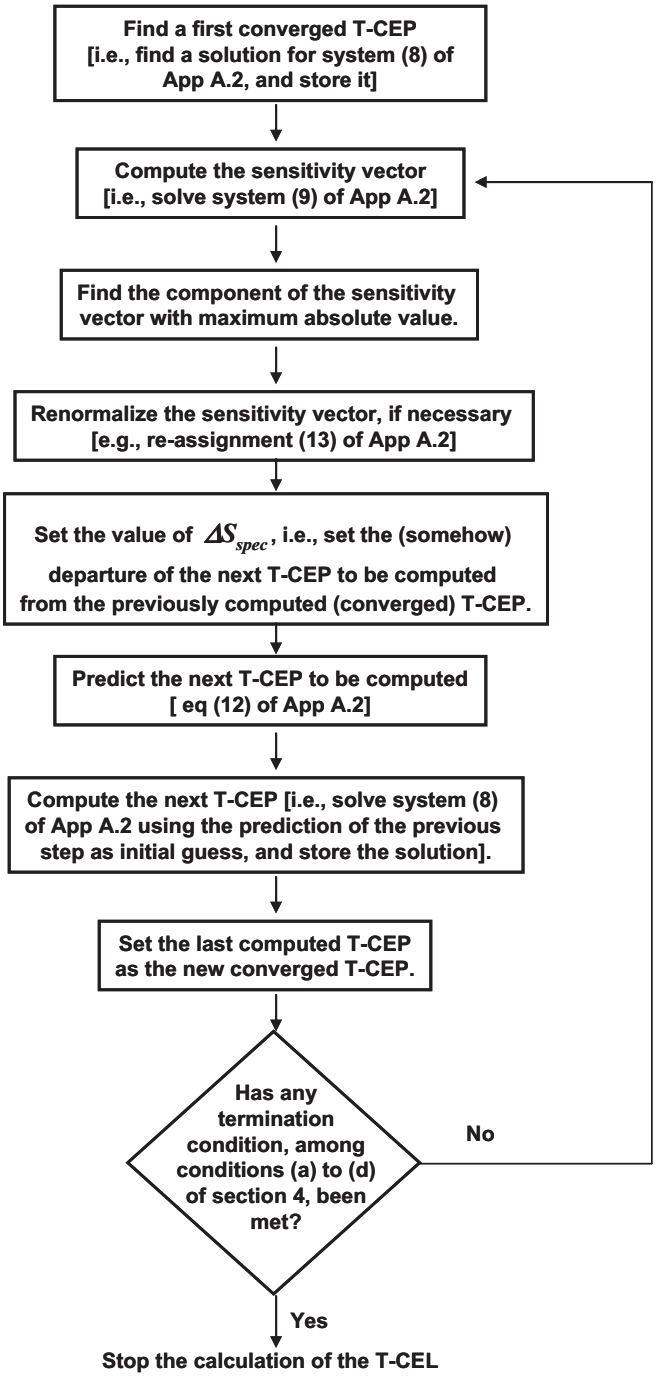

Fig. A.2.1. Procedure for computing a T-CEL

Appendix B. Additional results or projections of computed T-CELs

Figs. B.1 and B.2 show, for the system Carbon Dioxide + Water + 2-Propanol, the temperature (T)–molar volume (V) projection of lines T-CEL(a), T-CEL(g), T-CEL(h) and T-CEL(i) (see Fig. 2). Fig. B.2 is a zoom of Fig. B.1. Notice that, for the sake of clarity, the line T-CEL(b) is not shown in Figs. B.1 and B.2. In the T–V projection a T-CEL has two branches: one corresponding to the critical phase and the other to the non-critical phase. The T-CEL critical phase branch stems either from the critical phase of a B-CEP (e.g., empty circle at about 0.1 l/mol in Fig. B.1), or from the critical phase of a T-CEP-4PL (e.g., middle triangle at about 326 K in Fig. B.2, or rightmost triangle at about 333 K in Fig. B.2).

Figs. B.3 and B.4 (zoom of Fig. B.3) show a pressure–temperature projection for the system Ethane + Propane + n-Eicosane. The lines T-CEL(i) and T-CEL(ii) stem from the B-CEPs of the binary subsystem Ethane + n-Eicosane (see Table 2). Both T-CELs meet at a T-TCEP (type 8 in Table 1). Fig. B.4 shows more clearly the short binary critical line that goes from the pure ethane critical point (square) to the B-CEP at about 306.5 K (empty circle) of Ethane + n-Eicosane. The lines T-CEL(i) and T-CEL(ii) computed in this work agree qualitatively and quantitatively with the T-CELs calculated by Gregorowicz and de Loos [7]. Fig. B.5 shows the Pressure-molar volume projection for lines T-CEL(i) and T-CEL(ii). This projection is not shownin ref [7]. The leftmost circle at about 42 bar in Fig. B.5 is the critical phase of the lower CEP of the binary system Ethane + n-Eicosane. Hence, the critical branch of T-CEL(ii) is the left one. The rightmost circle at about 50 bar in Fig. B.5 is the critical phase of the upper CEP of the binary system Ethane + n-Eicosane. Therefore, the critical branch of T-CEL(i) is the one on the right.

Fig. B.6 shows a pressure-temperature projection of univariant lines for the system *ethane(1) + propane(2) + 1-propanol (3)*. The results correspond to the SRK-EOS with the following values for the interaction parameters: $k_{12} = 0$; $l_{12} = 0$; $k_{13} = 0$; $l_{13} = -0.15$; $k_{23} = -0.1$; $l_{23} = 0$. These parameter values imply the following phase behaviors for the binary subsystems [1]: *ethane(1) + propane(2)*: type I, *ethane(1) + 1-propanol (3)*: type II, and *propane(2) + 1-propanol (3)*: type I. The shown T-CEL originates at a B-CEP and extends indefinitely toward low pressures and low temperatures. This corresponds to type 1 in Table 1. Fig. B.7 shows a temperature-molar volume projection of the T-CEL of Fig. B.6,

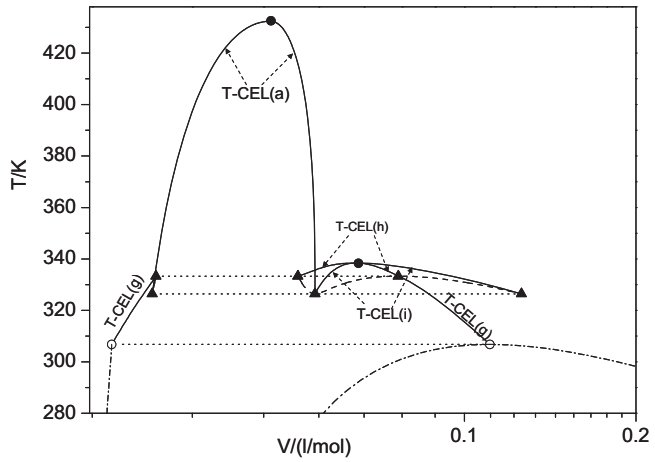

Fig. B.1. Calculated Temperature–Molar Volume projection of univariant lines of the system Carbon Dioxide + Water + 2 Propanol. Empty Circle: A phase of a Binary critical end point (B-CEP) of the $CO_2 + H_2O$ system. Triangle: A phase of a Ternary critical end point of a four phase line (T-CEP-4PL). Full Circle: Ternary tricritical end point (T-TCEP). Dashed Lines: Ternary four-phase equilibrium hyper-line. Dashed-dotted Lines: Phases of the Binary liquid–liquid–vapor equilibrium hyper-line (B-LLV). Dotted lines: auxiliary horizontal lines for easier visualization. The letters (a), (g), (h) and (i) are used to distinguish between the various T-CELs discussed in the text.

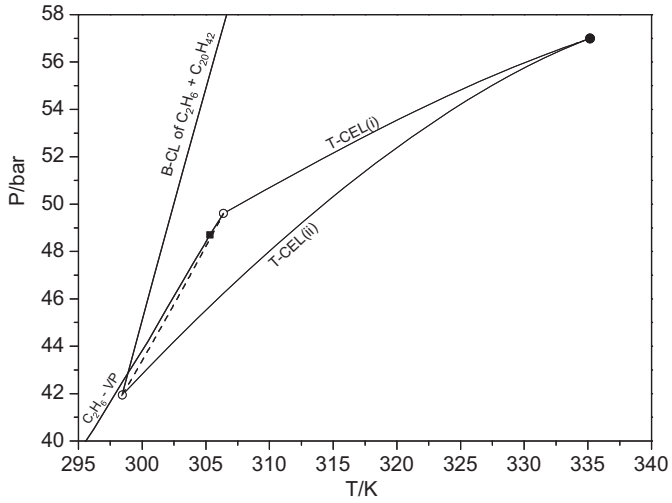

Fig. B.3. Calculated Pressure–Temperature projection of univariant lines of the system Ethane + Propane + n-Eicosane. Square: Critical point of pure C_2H_6. Empty circle: Binary critical end point (B-CEP) of system Ethane + n-Eicosane (type IV, Table 2). Full Circle: Ternary tricritical end point (T-TCEP). Dashed Line: Binary liquid–liquid–vapor equilibrium line (B-LLV). VP means "pure compound vapour–liquid equilibrium line". B-CL means "binary critical line". The letters (i) and (ii) are used to distinguish between the T-CELs discussed in the text.

together with the information on the three-phase equilibrium line of the binary subsystem *ethane(1) + 1-propanol (3)*.

Appendix C. Phenomenology of the fluid phase behavior of ternary mixtures seen on sets of Gibbs Triangles

The principles of phase equilibrium have been laid down essentially by Gibbs, Van der Waals and Bakhuis Roozeboom (se page 325 of ref [24]). Bakhuis Roozeboom and his school extensively studied, at the beginning of the 20th century, the phase equilibria of ternary mixtures including both, liquid and solid phases (ref [2], p. 128). The studies did not resort to thermodynamic models but considered Gibbsian thermodynamics in a phenomenological way [2]. The work of Bakhuis Roozeboom was continued (ref [24], p. 325) by several other authors up to ternary systems. Schreinemakers published, a hundred years ago, the third volume of the Bakhuis-Roozeboom series, which fully focused on ternary systems [2]. Unfortunately, Vol. III, and previous volumes, are practically no longer available [24].

The following discussion has the goal of facilitating the understanding of a significant part of the phenomenological behavior found in fluid ternary systems. We focus in particular on three and four-phase equilibria, on critical lines and on ternary critical end points (T-CEPs). What follows is mostly based on the comprehensive review by Adrian et al. [3].

Fig. C.1 shows the influence of pressure (p) on the phase equilibria of the system carbon dioxide (CO_2) + water (W) + (1-propanol) (1-POH) at 333 K. This figure was taken (and reproduced with additions) from ref [3]. Fig. C.1 is qualitative [3]. The right hand side

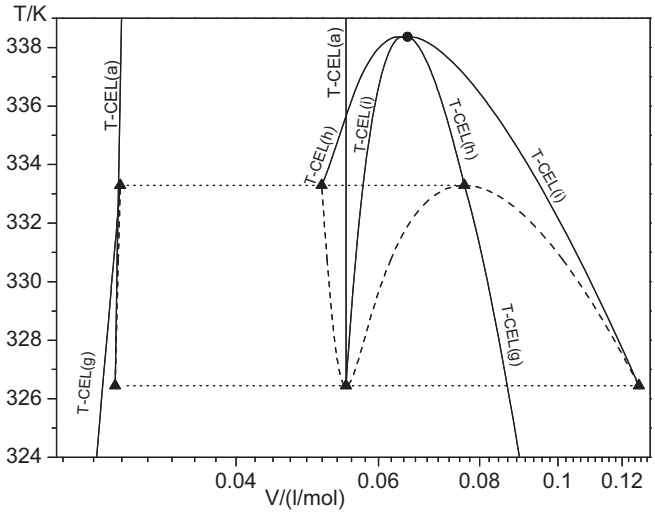

Fig. B.2. Zoom of Fig. B.1. Calculated Temperature–Molar Volume projection of univariant lines of the system Carbon Dioxide + Water + 2 Propanol. Triangle: A phase of a Ternary critical end point of a four phase line (T-CEP-4PL). Full Circle: Ternary tricritical end point (T-TCEP). Dashed Line: Ternary four-phase equilibrium line. Dotted lines: auxiliary horizontal lines for easier visualization. The letters (a), (g), (h) and (i) are used to distinguish between the various T-CELs discussed in the text.

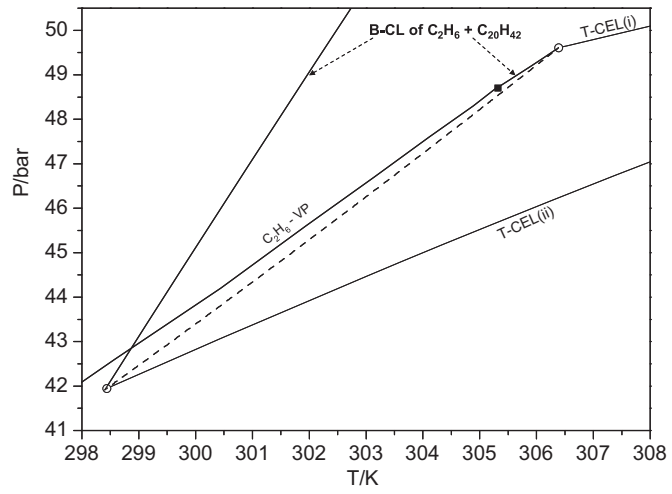

Fig. B.4. Zoom of Fig. B.3. Calculated Pressure–Temperature projection of univariant lines of the system Ethane + Propane + n-Eicosane. Square: Critical point of pure C_2H_6. Empty circle: Binary critical end point (B-CEP). Dashed Line: Binary liquid–liquid–vapor equilibrium line (B-LLV). VP means "pure compound vapour–liquid equilibrium line". B-CL means "binary critical line". The letters (i) and (ii) are used to distinguish between the T-CELs discussed in the text.

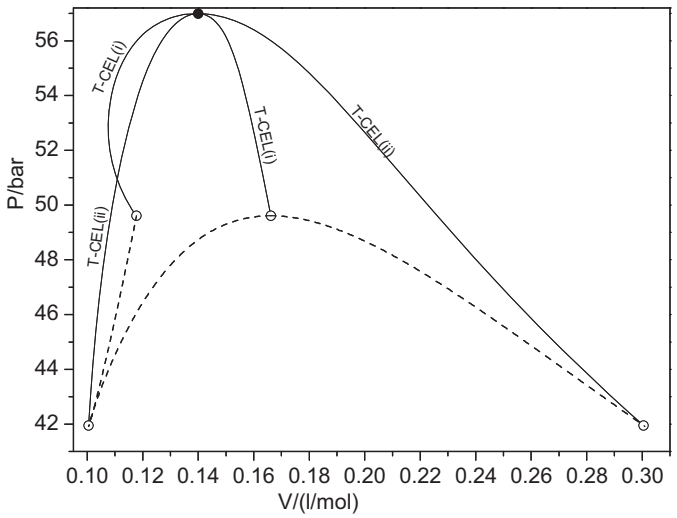

Fig. B.5. Calculated Pressure–Molar Volume projection of univariant lines of the system Ethane + Propane + n-Eicosane. Empty circle: A phase of the Binary critical end point (B-CEP) of system Ethane + n-Eicosane. Full Circle: Ternary tricritical end point (T-TCEP). Dashed Line: Binary three phase line. The letters (i) and (ii) are used to distinguish between the T-CELs discussed in the text.

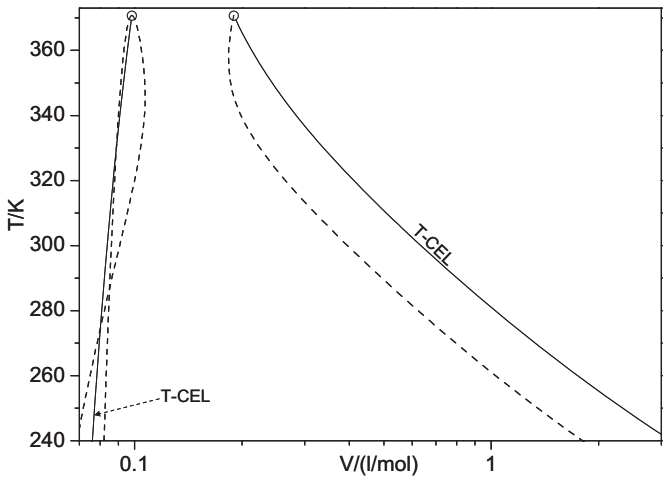

Fig. B.7. Calculated Pressure–Molar Volume projection of univariant lines of the system Ethane(1) + Propane(2) + 1 Propanol(3). Empty circle: A phase of the Binary critical end point (B-CEP) of Ethane(1) + 1-Propanol(3). Dashed Lines: phases of the Binary three phase equilibrium line. Model SRK-EOS with $k_{12} = 0$; $l_{12} = 0$; $k_{13} = 0$; $l_{13} = -0.15$; $k_{23} = -0.1$; $l_{23} = 0$.

of the figure shows the same prism diagram than the left hand side. It was included to clearly identify the phases at three-phase equilibrium as L1, L2 and V. The binary system CO_2 + W shows two-phase equilibria from pressure P1 to pressure P5. The system CO_2 + (1-POH) shows two-phase equilibria from P1 to a pressure less than P3, where it presents a critical point (point 6). At point 6 the binary liquid phase L2 becomes critical with the binary vapor phase V [$(L2 = V)_{CO2/(1\text{-}POH)}$]. The system W + (1-POH) is homogeneous throughout the pressure range of Fig. C.1. At P1 there is, for the ternary system, a single liquid–vapor (LV) region that connects the CO_2 + W side and the CO_2 + (1-POH) side of the Gibbs triangle.

At pressure P2 there is a liquid–liquid–vapor (L1L2V) region, represented by the shaded triangle. From the L2V side of the shaded triangle a ternary two-phase region (which we name L2V two-phase region) arises. It ends at the CO_2 + (1-POH) side of the Gibbs triangle. A similar situation occurs for the L1V side of the shaded triangle from which the L1V two-phase region originates and extends up to the CO_2 + W side of the Gibbs triangle. A third two-phase region originates at the L1L2 side of the shaded triangle. Such L1L2 two-phase region ends a the ternary critical point labeled "4", where phases L1 and L2 become identical.

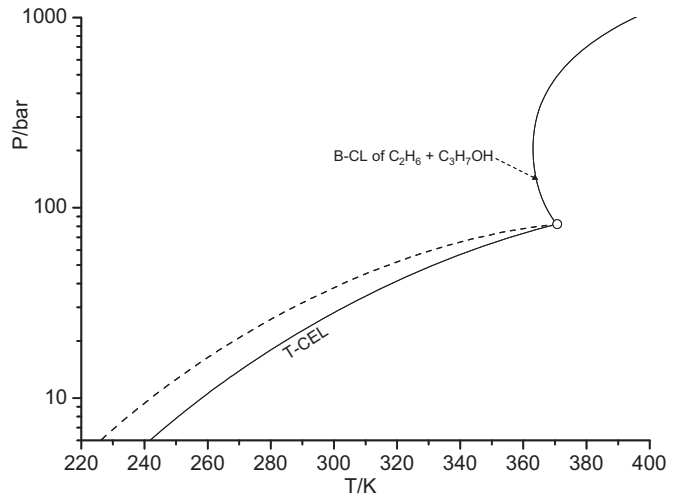

Fig. B.6. Calculated Pressure–Temperature projection of univariant lines of the system Ethane(1) + Propane(2) + 1 Propanol(3). Empty circle: Binary critical end point (B-CEP). Dashed Line: Binary three phase equilibrium line. Model SRK-EOS with $k_{12} = 0$; $l_{12} = 0$; $k_{13} = 0$; $l_{13} = -0.15$; $k_{23} = -0.1$; $l_{23} = 0$. B-CL means "binary critical line".

At pressure P3 the system also presents a three-phase equilibrium region. Now the L1L2 two-phase region is larger in size and has the critical point "3", while the L2V two-phase region has reduced its size and has a critical point (labeled "7"). This region has an even lower size at P4, and also has the critical point 8. At the pressure of point 9, the L2V two-phase region reaches a zero-size, i.e. the phases L2 and V become critical (L2 = V), while remaining at equilibrium with phase L1 [L1(L2 = V)]. This situation, where two of the phases at three-phase equilibria become critical, corresponds to a ternary critical endpoint (T-CEP, point 9). Point 9 only shows the composition of the critical phase of the T-CEP. The composition of the non-critical phase at equilibrium with the critical phase (point 9) would be similar to the composition of phase L1 at P4. Notice that point 9 is an endpoint of the dashed line that connects the critical points 6, 7 and 8. We name such line as "6-9 line". Since it connects a continuous set of critical points, the "6-9 line" is a ternary (isothermal) critical line. The "6-9 line" (actually a critical hyper-line) belongs to a critical hyper-surface. The reader willing to visualize a projection [i.e., the pressure/temperature/solvent-free composition projection] of a ternary critical hyper-surface might want to consult ref [4] (page 135). At point 9 the critical line becomes globally unstable, i.e., the critical phase (L2 = V) is at equilibrium with the non-critical L1 phase [L1(L2 = V)]. Actually, a given point of the "6-9 line" is described by more coordinates than those shown in Fig. C.1. One of such (not shown) coordinates is the molar volume of the critical phase. In other words, since it exists in a multi-dimensional space, the critical "6-9 line" is actually a hyper-line. The prefix "hyper" means, in this work, "existing in a space with more than three dimensions". The critical conditions written for a ternary system lead to the conclusion that a ternary critical point has two degrees of freedom. This means that ternary systems have critical surfaces (or hyper-surfaces). Clearly, the critical "6-9 line" is the result of intersecting a ternary critical hyper-surface with an isothermal hyper-plane at 333 K. A ternary three-phase equilibrium also has two-degrees of freedom. Therefore, ternary systems showing three-phase equilibria have three-phase hyper-surfaces. A continuous set of ternary three-phase equilibria at constant temperature is a three-phase hyperline resulting from the intersection

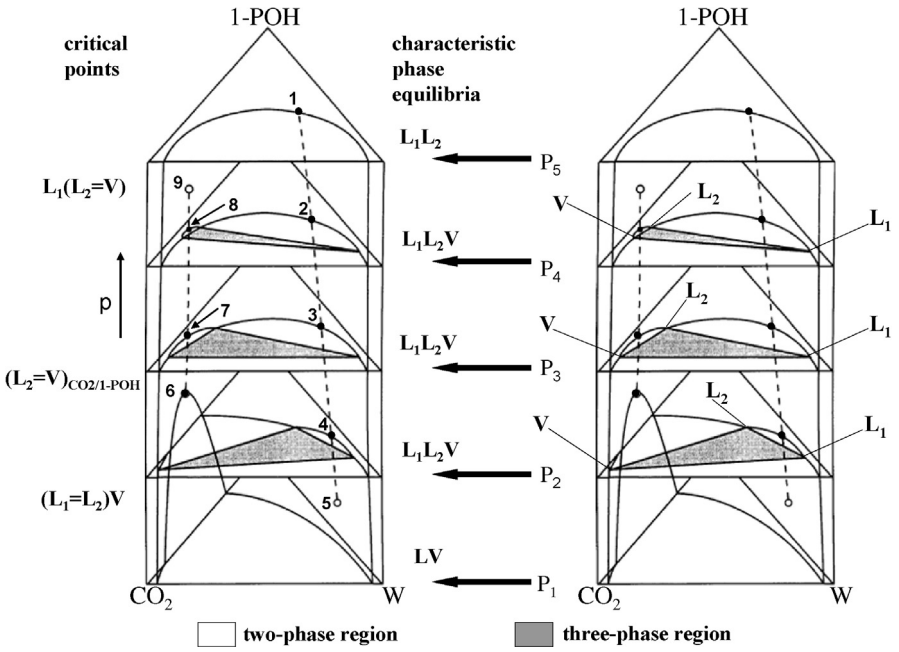

Fig. C.1. The influence of pressure on the phase equilibria of the system carbon dioxide + water + (1-propanol) at 333 K. This figure was adapted with permission from Fig. 4 of ref [3]

of a ternary three-phase hyper-surface and an isothermal hyper-plane. To fix ideas, the three shaded triangles in Fig. C.1 belong to an isothermal three-phase hyperline at 333 K. This hyper-line ends at the T-CEP labeled "9". In conclusion, at a T-CEP a three-phase hyper-line and a critical hyperline meet. This same phenomenon is the one that occurs at binary critical endpoints. The fact that ternary three-phase and critical hyper-lines meet at a T-CEP implies that ternary three-phase and critical hyper-surfaces meet at a line of T-CEPs. Such line is named ternary critical end line (T-CEL) in this work. It sets the end of both, a critical hyper-surface and a three-phase hyper-surface which meet at the T-CEL.

Fig. C.1 also shows a critical line that connects the critical points 1, 2, 3, 4 and 5. Such line ends at the T-CEP labeled "5" where phases L1 and L2 become critical, while being at equilibrium with the non-critical phase V [(L1 = L2)V]. Notice that the three-phase hyper-line of Fig. C.1 has two T-CEPs: one of them at high pressure ($P_{T\text{-}CEP} > P4$, point 9) and the other at low pressure ($P1 < P_{T\text{-}CEP} < P2$, point 5). The T-CEPs 5 and 9 set the pressure range of existence of the isothermal (333 K) three-phase hyper-line. Notice that beyond the pressures of points 5 and 9 only single two-phase regions exist, at 333 K.

Fig. C.2 was also taken (and also reproduced with additions) from ref [3]. Fig. C.2 shows a phase behavior more complex than that of Fig. C.1. The system is the same for Figs. C.1 and C.2. At the temperature (298 K) of Fig. C.2, the CO_2 + W binary subsystem presents a liquid–vapor region at low pressure, a liquid–liquid region at high pressure, and a second small vapor–liquid region that originates at the pure CO_2 vapor–liquid equilibrium point at 298 K. The three CO_2 + W fluid-fluid equilibrium regions meet at a liquid–liquid–vapor point. This happens at pressure P6. At pressure P4 in Fig. C.2, we see a ternary four-phase equilibrium (4PE) represented as an irregular black quadrilateral (=tetragon = quadrangle) in the Gibbs triangle. The four phases at equilibrium have the labels L1, L2, L3 and V. The two-phase region L1L2 originates at the L1L2 side of the tetragon and ends at the critical point "5". Analogously, there is a L2L3 two-phase region stemming from the L2L3 side of the quadrangle which ends at the "*e*" critical point. There are two additional ternary two-phase regions at pressure P4: (a) one of them goes from the L3V side of the quadrilateral to the liquid–vapor part of the binary CO_2 + (1-POH) side of the Gibbs triangle, and, (b), the other two-phase region connects the L1V tetragon side to the liquid–vapor part of the CO_2 + W side of the Gibbs triangle. There are two single phase regions at pressure P4. One of them includes the pure W and pure 1-POH vertices. The second one is small in size and includes the CO_2 vertex.

The four-phase equilibrium at pressure P4 becomes split into two three-phase equilibria at pressure P5. Such equilibria are separated by a L1L3 two-phase region. Notice that the nature of the phases of the $L1^*L2L3$ three-phase equilibrium at P5 is the same than the nature of the phases that remain after removing the vapor phase V from the tetragon at P4. Similarly, after removing phase L2 from the quadrangle at P4, we obtain a set of three phases having the same nature than the phases $L1L3^*V$ of the three-phase equilibrium at P5. In other words, the two three-phase regions at P5 can be seen as coming from having divided the quadrilateral at P4 into two parts, being the dividing line the diagonal L1L3. Analogously, the two three-phase regions at P3 come from cutting the quadrangle at P4, along the L2V diagonal.

The $L2^*L3V^*$ locus that exists at pressures less than P4 ends at point "g", which is a T-CEP. Fig. C.2 also shows a L1L2V locus at pressures less than P4 which ends at the T-CEP "8". On the other hand, the $L1L3^*V$ locus happens at pressures greater than P4, as it is the case for the $L1^*L2L3$ locus. The $L1L3^*V$ locus ends at the binary CO_2 + W liquid–liquid–vapor point that happens at P6. Finally, the $L1^*L2L3$ locus ends at the T-CEP "*a*". Notice that Fig. C.2 shows four three-phase loci, i.e., the loci $L2^*L3V^*$, L1L2V, $L1L3^*V$ and $L1^*L2L3$. Each locus is a different three-phase equilibrium hyper-line. Therefore, four different three-phase equilibrium hyper-lines arise from the four-phase equilibrium hyper-point at P4. Two out of the four three-phase equilibrium hyper-lines exist (i.e., are globally stable) at pressures greater than P4, while the other two three-phase equilibrium hyper-lines exist at pressures less than P4. To fix ideas, Table C.1 specifies the endpoints for the four three-phase loci.

At pressure P7 there are three two-phase regions: one of them has the critical point "*2*", another (small) one has the critical point "*b*", and the last one ends at the two-phase part of the binary CO_2 + W side of the Gibbs triangle. At the T-CEP "*a*" the three two-phase regions have become a single two-phase region. This condition remains at higher pressures, e.g., at P8. With regard to

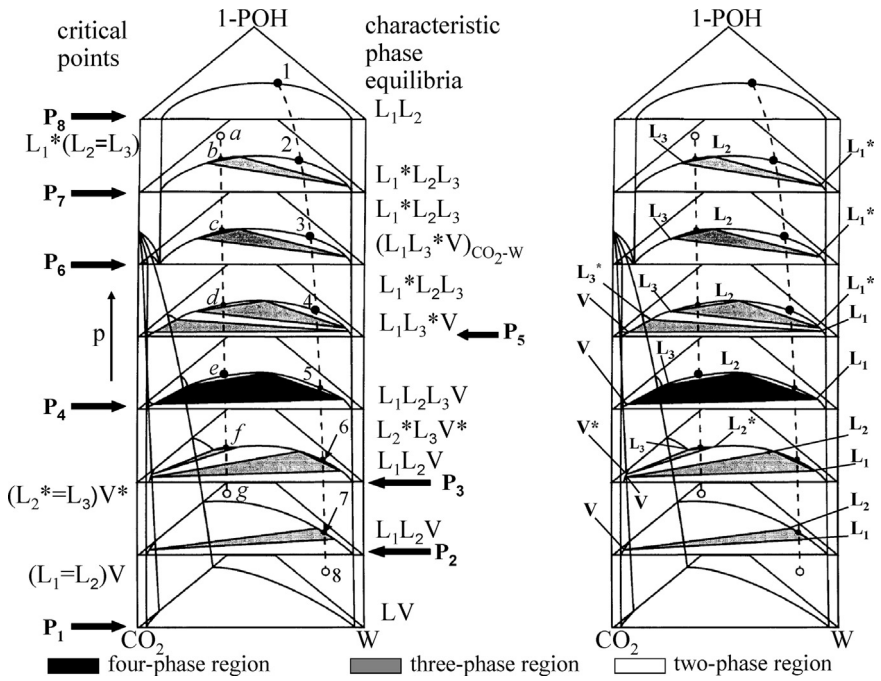

Fig. C.2. The influence of pressure on the phase equilibria of the system carbon dioxide + water + (1-propanol) at 298 K. This figure was adapted with permission from Fig. 5 of ref [3].

Table C.1
End points of the three-phase equilibrium loci of Fig. C.2.

Locus	Lower pressure endpoint	Higher pressure endpoint
L2*L3V*	T-CEP "g"	4PE at pressure P4
L1L2V	T-CEP "8"	4PE at pressure P4
L1L3*V	4PE at pressure P4	Binary CO_2 + W liquid–liquid–vapor point
L1*L2L3	4PE at pressure P4	T-CEP "a"

the T-CEP "g", the situation is analogous to that of the T-CEP "*a*". However the fusion of the three two-phase regions into a single one happens when pressure is decreased (not increased) up to the pressure at point "g". Although pressure P2 is below the pressure of the T-CEP "g", we still see a three phase equilibrium point (L1L2V) at such pressure. Therefore it would be wrong to state that beyond a T-CEP three-phase equilibria do not exist. Otherwise, all that we would assure is that beyond a T-CEP three-phase equilibria do not exist at conditions sufficiently close to those of the T-CEP. We mean by "conditions sufficiently close to those of the T-CEP" both, that the temperature and the pressure are close enough to those of the T-CEP, and that the overall composition is close enough to a point of the T-CEP tie-line. Such tie-line connects the T-CEP critical phase with the T-CEP non-critical phase. This can be concisely summarized as follows: at a T-CEP one three-phase equilibrium region ceases to exist.

Interestingly, the critical line which connects the points [*a,b,c,d,e,f,g*] links continuously the T-CEP of locus L1*L2L3, i.e., point "*a*" with the T-CEP of locus L2*L3V*, i.e., point "*g*". This happens in spite of the fact that the loci L1*L2L3 and L2*L3V* differ, in a way, in their nature. In other words, although the pressure of the four-phase equilibrium, i.e., P4, is an endpoint pressure for loci L1*L2L3 and L2*L3V*, it is not and endpoint pressure for the [*a,b,c,d,e,f,g*] critical locus. This is to say that the critical locus somehow crosses over the four-phase equilibrium hyper-point, while none of the four three-phase loci do. The situation is the same for the critical locus that connects the points 1 to 8.

In spite of its complexity, the phase behavior shown in Figs. C.1 and C.2 does not encompass all the possibilities at all (e.g., ternary azeotropic behavior). For instance, Michelsen and Mollerup [20] have shown a figure (their figure 13 on page 325) corresponding to a calculated ternary phase diagram represented in a Gibbs triangle at set temperature and pressure. The diagram presents five separate two-phase regions, two separate three-phase regions, and three separate single phase regions, one of which is small and of the "island" type. This last (unusual) single-phase region reaches none of the binary sides of the Gibbs triangle.

More information on the phenomena represented in Figs. C.1 and C.2 can be found in ref [3] where the physical mechanisms behind the phase behavior shown in Figs. C.1 and C.2 are discussed in detail.

References

[1] R.L. Scott, P.H. Van Konynenburg, Static properties of solutions: Van der Waals and related models for hydrocarbon mixtures, Discussions of the Faraday Society 49 (1970) 87–97.
[2] J. Levelt Sengers, How fluids unmix, Discoveries by the School of Van der Waals and Kamerlingh Onnes, Edita Knaw, Amsterdam.
[3] T. Adrian, M. Wendland, H. Hasse, G. Maurer, High-pressure multiphase behaviour of ternary systems carbon dioxide-water-polar solvent: review and modeling with the Peng-Robinson equation of state, The Journal of Supercritical Fluids 12 (1998) 185–221.
[4] K. Gauter, C.J. Peters, A.L. Scheidgen, G.M. Schneider, Cosolvency effects, miscibility windows and two-phase lg holes in three-phase llg surfaces in ternary systems: a status report, Fluid Phase Equilibria 171 (2000) 127–149.
[5] J.R. Di Andreth, Multiphase Behavior, In Ternary Fluid Mixture, Ph.D. Thesis, Deparment of Chemical Engineering, University of Delaware, Delaware, USA, 1985, p. 164.
[6] D.-Y. Peng, D.B. Robinson, A new two-constant equation of state, Industrial & Engineering Chemistry Fundamentals 15 (1976) 59–64.
[7] J. Gregorowicz, T.W. de Loos, Modelling of the three phase LLV region for ternary hydrocarbon mixtures with the Soave-Redlich-Kwong equation of state, Fluid Phase Equilibria 118 (1996) 121–132.
[8] T. Adrian, S. Oprescu, G. Maurer, Experimental investigation of the multiphase high-pressure equilibria of carbon dioxide-water-(1-propanol), Fluid Phase Equilibria 132 (1997) 187–203.
[9] S. Winkler, K. Stephan, Fluid multiphase behavior in ternary mixtures of CO2, H2O and 1-butanol, Fluid Phase Equilibria 137 (1997) 247–263.
[10] G. Soave, Equilibrium constants from a modified Redlich-Kwong equation of state, Chemical Engineering Science 27 (1972) 1197–1203.
[11] K. Chobanov, D. Tuma, G. Maurer, High-pressure phase behavior of ternary systems (carbon dioxide + alkanol + hydrophobic ionic liquid), Fluid Phase Equilibria 294 (2010) 54–66.

[12] T. Ulanova, D. Tuma, G. Maurer, High-pressure multiphase behavior of the ternary systems (ethene + water + acetone) and (ethane + water + acetone), Journal of Chemical and Engineering Data 55 (2010) 4450–4462.
[13] T. Ulanova, D. Tuma, G. Maurer, Salt effect on the high-pressure multiphase behavior of the ternary system (Ethene + Water + 2-Propanol)†, Journal of Chemical & Engineering Data 54 (2008) 1417–1420.
[14] J. Freitag, M.T. Sanz Díez, D. Tuma, T.V. Ulanova, G. Maurer, High-pressure multiphase behavior of the ternary systems (ethene + water + 1-propanol) and (ethene + water + 2-propanol): Part I: Experimental investigation, The Journal of Supercritical Fluids 32 (2004) 1–13.
[15] J. Freitag, D. Tuma, T.V. Ulanova, G. Maurer, High-pressure multiphase behavior of the ternary systems (ethene + water + 1-propanol) and (ethene + water + 2-propanol) Part II: modeling, The Journal of Supercritical Fluids 39 (2006) 174–186.
[16] M. Bluma, U.K. Deiters, A classification of phase diagrams of ternary fluid systems, Physical Chemistry Chemical Physics 1 (1999) 4307–4313.
[17] M.L. Michelsen, Calculation of critical points and phase boundaries in the critical region, Fluid Phase Equilibria 16 (1984) 57–76.
[18] M. Cismondi, M.L. Michelsen, Global phase equilibrium calculations: critical lines, critical end points and liquid-liquid-vapour equilibrium in binary mixtures, Journal of Supercritical Fluids 39 (2007) 287–295.
[19] E.L. Allgower, K. Georg, in: Introduction to Numerical Continuation Methods, SIAM, Classics in Applied Mathematics, Philadelphia, 2003.
[20] M.L. Michelsen, J.M. Mollerup, Thermodynamic Models: Fundamentals and Computational Aspects, Tie-Line Publications, Holte, 2007, pp. 231–249.
[21] I. Polishuk, J. Wisniak, H. Segura, Estimation of Liquid – Liquid – Vapor equilibria in binary mixtures of n-alkanes, Industrial & Engineering Chemistry Research 43 (2004) 5957–5964.
[22] H. Segura, T. Kraska, A. Mejía, J. Wisniak, I. Polishuk, Unnoticed pitfalls of soave-type alpha functions in cubic equations of state, Industrial & Engineering Chemistry Research 42 (2003) 5662–5673.
[23] R.L. Rowley, W.V. Wilding, J.L. Oscarson, Y. Yang, N.A. Zundel, T.E. Daubert, R.P. Danner, in: DIPPR Data Compilation of Pure Compound Properties, Design Institute for Physical Properties, AIChE, New York, 2003.
[24] R. Koningsveld, W.H. Stockmayer, E. Nies, in: Polymer Phase Diagrams: A Textbook, Oxford University Press, New York, 2001.
[25] J.R. Di Andreth, M.E. Paulaitis, An experimental study of three- and four-phase equilibria for isopropanol—water—carbon dioxide mixtures at elevated pressures, Fluid Phase Equilibria 32 (1987) 261–271.
[26] A.L. Scheidgen, G.M. Schneider, Fluid phase equilibria of (carbon dioxide + a 1-alkanol + an alkane) up to 100 MPa and T = 393 K: cosolvency effect, miscibility windows, and holes in the critical surface, The Journal of Chemical Thermodynamics 32 (2000) 1183–1201.

The Journal of Supercritical Fluids

Editor-in-Chief's Featured Article

May 2014

Awarded to:

G. Pisoni, M. Cismondi, L. Cardozo-Filho, M.S. Zabaloy

For the Article:

Critical end line topologies for ternary systems

Volume 89, May 2014, Pages 33-47

Angela Welch, Ph.D
Senior Publisher

Professor Erdogan Kiran
Editor-in-Chief